Properties of the Eigenstates of Graphene Billiards: A comparison with Relativistic and Nonrelativistic Quantum Billiards

- Quantum Chaos $\rightarrow$ Classical Billiards, Quantum Billiards (QB), Neutrino Billiards (NB) , Graphene Billiards (GB)
- Experiments with Superconducting Microwave Billiards Simulating Artificial Graphene

Collaborators: Weihua Zhang (Lanzhou University + PCS IBS Daejeon)

Experiments:

@ TU Darmstadt: Achim Richter, Maksym Miski Oglu, Tobias Klaus

@ Lanzhou University: Weihua Zhang, Xiaodong Zhang, Jiongning Che

Classical Billiards with Integrable & Chaotic Dynamics

Rectangular billiard (integrable)

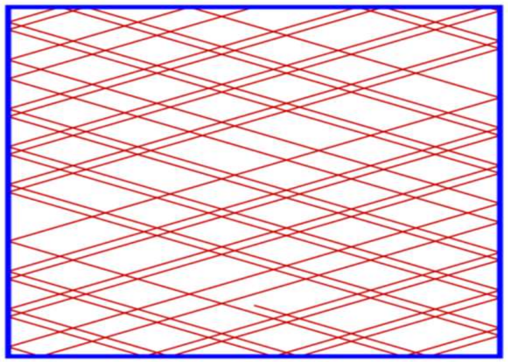

Africa billiard (chaotic)

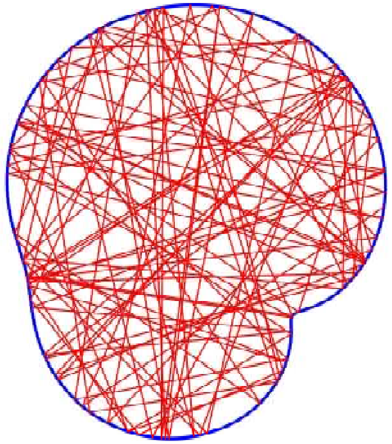

- Particle moves freely within the billiard along straight lines with constant velocity and is reflected specularly at boundary
- Classical dynamics is determined by the shape of the billiard

$\rightarrow$ Paradigm model for studies in the field of quantum chaos

- Central question in quantum chaos:

  How does the regular or chaotic behaviour of the classical dynamics manifest itself in the corresponding quantum system?

One Aspect of Quantum Chaos: Statistical Properties of the Eigenstates

- *Nonrelativistic Quantum Systems*
- Berry-Tabor Conjecture: The spectral fluctuation properties of generic integrable systems coincide with those of uncorrelated random numbers from a Poisson process
- Bohigas-Gianonni-Schmit Conjecture (1984) [Casati et al. (1980)]: The spectral fluctuation properties of generic classically chaotic quantum systems with preserved / violated time-reversal invariance coincide with those of random matrices from the Gaussian Orthogonal (GOE) / Gaussian Unitary (GUE) Ensemble
- *Relativistic Quantum Systems*

→ Question: Do the conjectures apply to relativistic neutrino billiards?
→ Problem: NBs do not have a well-defined classical limit
→ Semiclassical approach: Trace formula and Husimi functions

Wave Equation of Quantum Billiards

- Schrödinger equation for quantum billiard

Energy spectrum

Wave functions

$$\left(\frac{\hbar^2}{2m}\Delta + E\right)\Psi = 0, \qquad \Psi\big|_{\partial\Omega} = 0 \longrightarrow$$

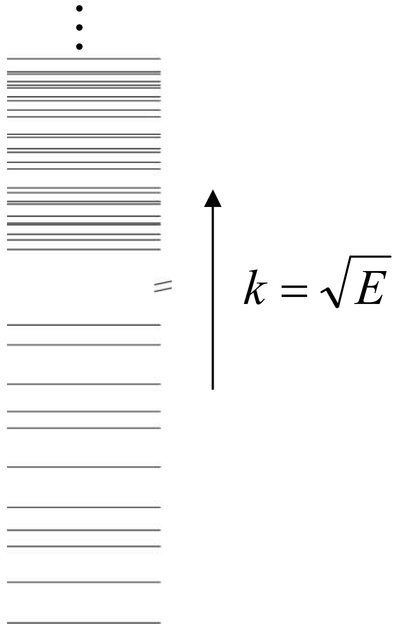

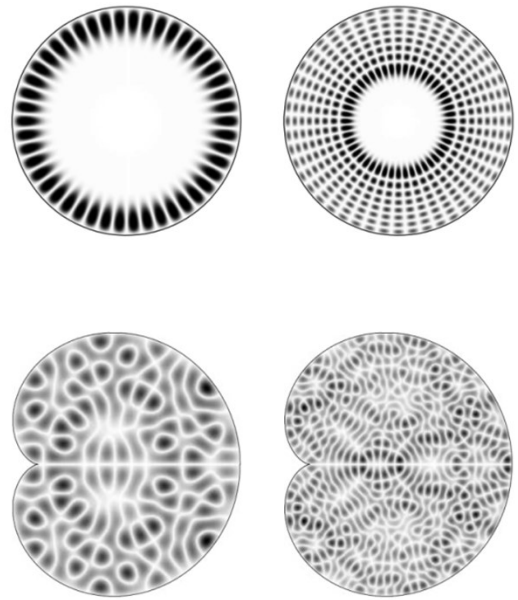

- Unfolding to energy-independent spectral density / mean spacing needed to identify universal fluctuation properties
- Weyl formula for QBs: $\overline{N}\left(k = \sqrt{E}\right) = N^{Weyl}(k) = \frac{A}{4\pi}k^2 - \frac{U}{4\pi}k + const.$

Dirac Equation for Neutrino Billiards

Berry & Mondragon, Proc. R. Soc. Lond. A 412, 53 (1987)

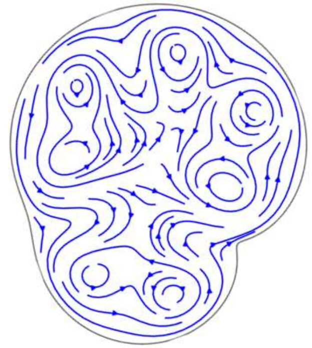

- Dirac equation for massive NB

$$\hat{H}_D\boldsymbol{\psi} = \left(c\hat{\boldsymbol{\sigma}}\cdot\hat{\boldsymbol{p}} + mc^2\hat{\boldsymbol{\sigma}}_{\boldsymbol{z}}\right)\boldsymbol{\psi} = E\boldsymbol{\psi},\ \boldsymbol{\psi} = \begin{pmatrix}\psi_1\\ \psi_2\end{pmatrix}$$

- BC requires that the outward current vanishes along boundary

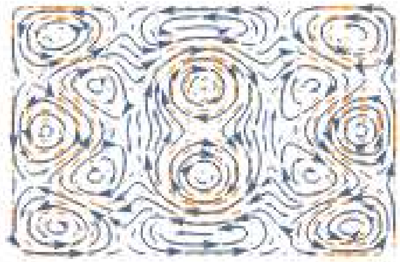

$$\mathbf{n}\cdot\left[\boldsymbol{\psi}^{\dagger}\boldsymbol{\nabla}_{\boldsymbol{p}}\hat{\boldsymbol{H}}_D\boldsymbol{\psi}\right] = 0$$

- Complex-plane presentation: $w(s)=x(s)+\mathrm{i}y(s)$, $\mathbf{n}=e^{\mathrm{i}\alpha(s)}$

- BC links the spinor components at the boundary

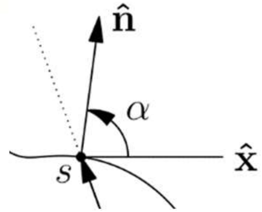

$$\psi_2(s) = ie^{i\alpha(s)}\psi_1(s)$$

- The Dirac equation for neutrino billiards is not time-reversal invariant

$\Rightarrow$ The spectral properties of typical NBs with shapes of chaotic billiards agree with GUE

Dirac Equation for Massive Neutrino Billiards

- The energy E is given in terms of the free space wavevector k as

$$E = \hbar c k_E = \hbar c k \sqrt{1+\beta^2},\ \beta = \frac{mc}{\hbar k}$$

- Define

$$\psi = \begin{pmatrix} \sqrt{\frac{1+\sin\theta_\beta}{2}}\tilde{\psi}_1 \\ \sqrt{\frac{1-\sin\theta_\beta}{2}}\tilde{\psi}_2 \end{pmatrix} \qquad \sin\theta_\beta = \frac{\beta}{\sqrt{1+\beta^2}}.$$

nonrel. Limit $\Leftrightarrow$ $\theta_\beta \to \pi/2$
ultrarel. Limit $\Leftrightarrow$ $\theta_\beta \to 0$

$$\Rightarrow\ k\tilde{\boldsymbol{\psi}}(\boldsymbol{r}) + i\hat{\boldsymbol{\sigma}}\cdot\nabla\tilde{\boldsymbol{\psi}}(\boldsymbol{r}) = 0 \quad \text{with} \quad \tilde{\psi}_2(s) = i e^{i\alpha(s)}\mathcal{K}^{-1}\tilde{\psi}_1(s) \qquad \mathcal{K} = \sqrt{\frac{1-\sin\theta_\beta}{1+\sin\theta_\beta}}$$

- The nonrelativistic limit $\beta \to \infty$ for fixed $\hbar k_{max}$ complies with the BC

- Weyl formula: $$\overline{N}\left(k=\sqrt{E}\right) = N^{Weyl}(k) = \frac{A}{4\pi}k^2 \cancel{-\frac{U}{4\pi}k} + const.$$

Statistical Measures for the Spectral Fluctuations

- Short-range correlations:
- NNSD: distribution of the spacings between adjacent levels

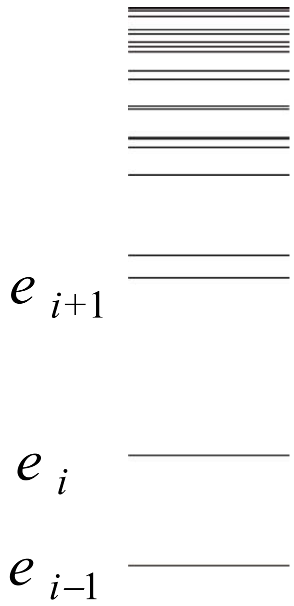

- Integrable systems: $$P^{\mathrm{Poi}}(s) = e^{-s}$$

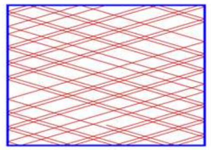

- Chaotic systems: $$P^{\mathrm{GOE}}(s) = \frac{\pi}{2} s e^{-\frac{\pi}{4}s^2}$$

$$P^{\mathrm{GUE}}(s) = \frac{32}{\pi^2} s^2 e^{-\frac{4}{\pi}s^2}$$

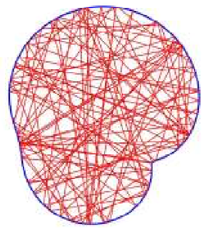

- Distribution of the ratios of two consecutive spacings of nearest-neighbors

Poisson: $\mathcal{P}_0(r) = 1/(1+r)^2$ GEs: $P_W(r) = \frac{1}{Z_\beta} \frac{(r+r^2)^\beta}{(1+r+r^2)^{1+(3/2)\beta}}$

- Long-range correlations:
- Number variance $\Sigma^2(L)$: $\Sigma^2(L) = <(N(L) - <N(L)>)^2>$

Center for Theoretical Physics of Complex Systems

Spectral Properties of the Rectangular & Africa NB & QB

Rectangular billiard

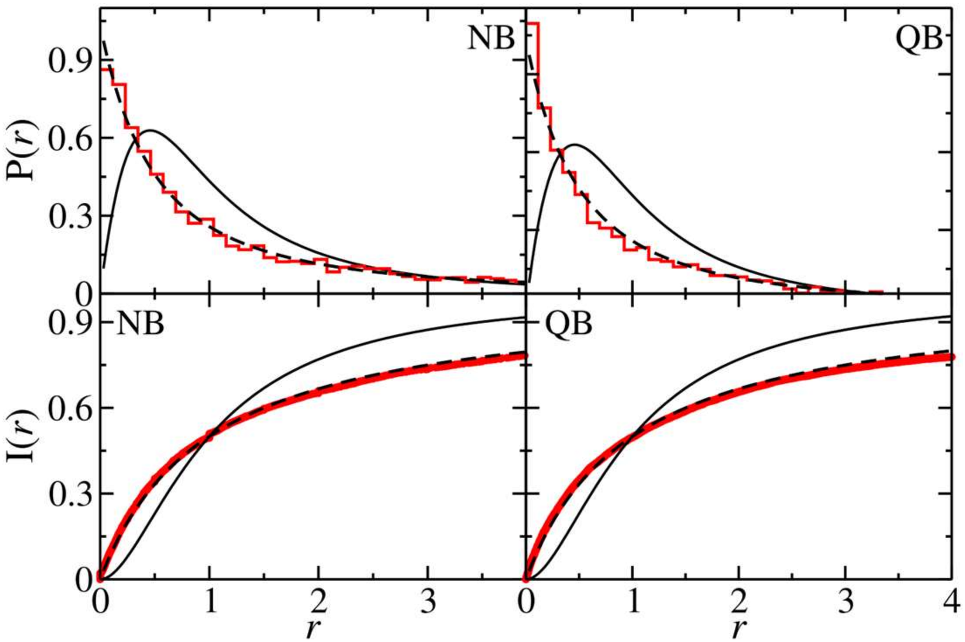

Africa billiard

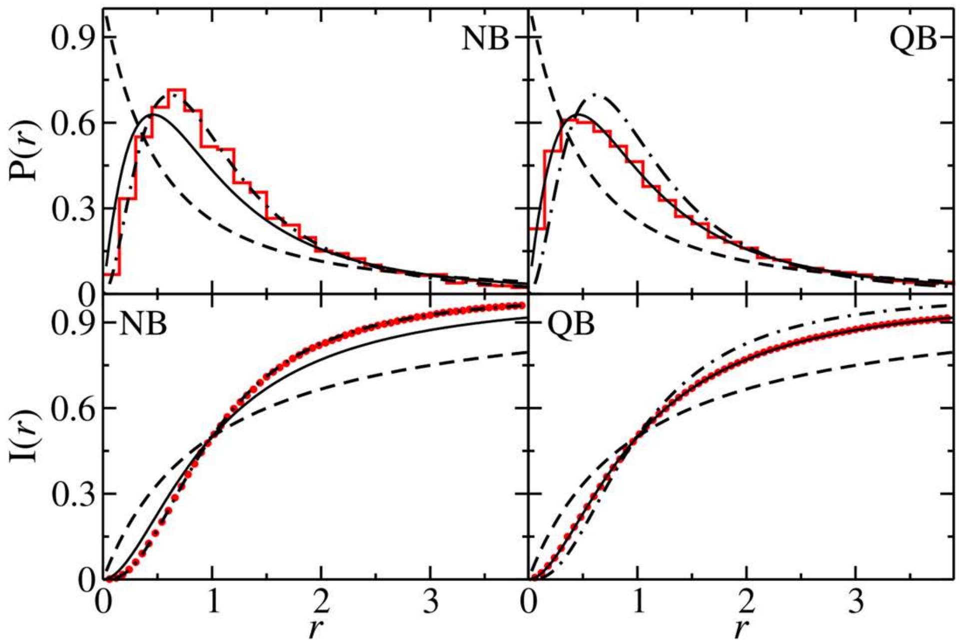

- The spectral properties of the rectangular QB & NB coincide with Poisson
- Africa QB $\rightarrow$ GOE
- Africa NB $\rightarrow$ GUE

Graphene

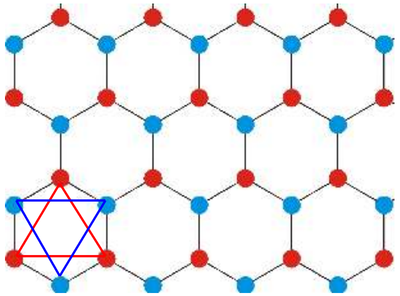

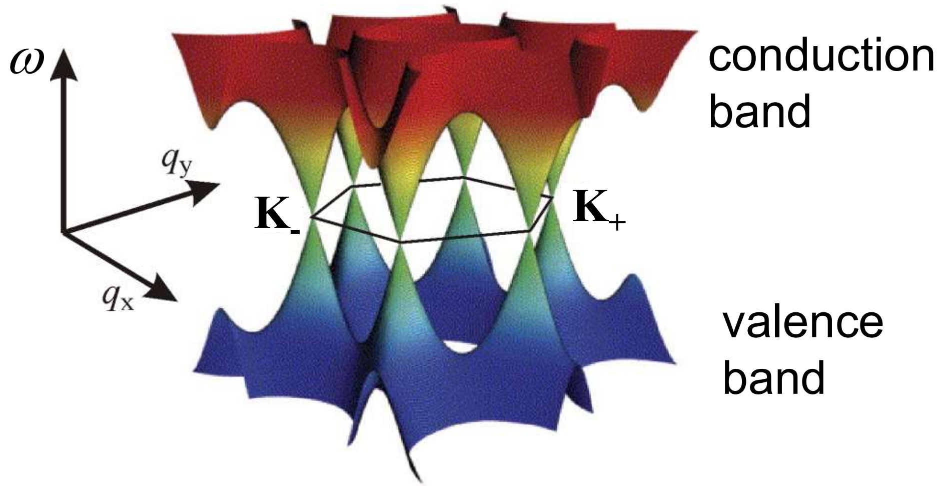

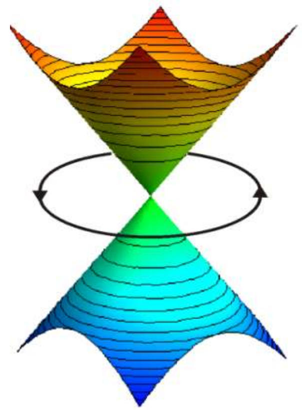

- Near each corner of the first hexagonal Brillouin zone the electron energy ω exhibits a linear dependence on the quasimomentum q
- Close to the diabolical ('Dirac') points the band structure is described by the Dirac equation of massless fermions

$$\pm \begin{pmatrix} 0 & \partial_x - i\partial_y \\ \partial_x + i\partial_y & 0 \end{pmatrix} \begin{pmatrix} \Psi_A \\ \Psi_B \end{pmatrix} = i\frac{\omega - \omega_D}{v_F} \begin{pmatrix} \Psi_A \\ \Psi_B \end{pmatrix}$$

- Independent contributions from K_+ and K_- valleys $\Rightarrow$ 4D Dirac equation

Graphene Billiards

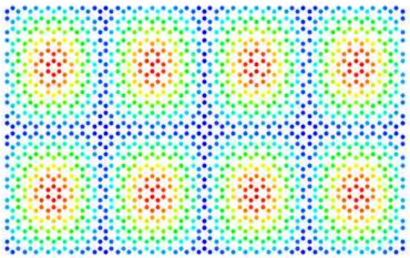

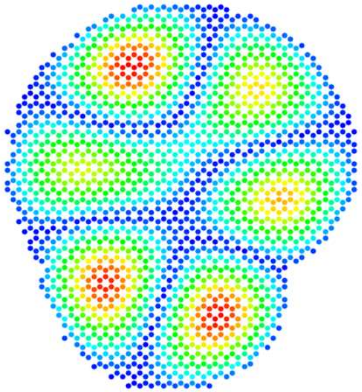

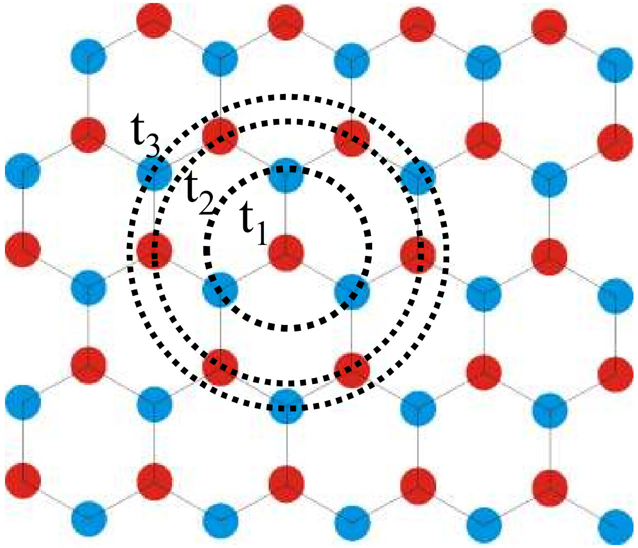

- Qualitative and quantitative insight is obtained with the tight-binding model

$$\hat{\mathcal{H}}_{ij}^{TBM} = t_0\delta_{ij} + t_1\delta(|\boldsymbol{r}_i - \boldsymbol{r}_j| - d_0) + t_2\hat{\delta}(|\boldsymbol{r}_i - \boldsymbol{r}_j| - d_1) + \ldots..$$

- Assumption: interaction of the graphene p_z orbitals non-negligible for 1st, 2nd and 3rd nearest neighbors
- Electrons cannot escape from a graphene flake $\leftrightarrow$ Dirichlet BCs along the 1st missing row of atoms outside sheet

Spectral Density of the Africa Graphene Billiard

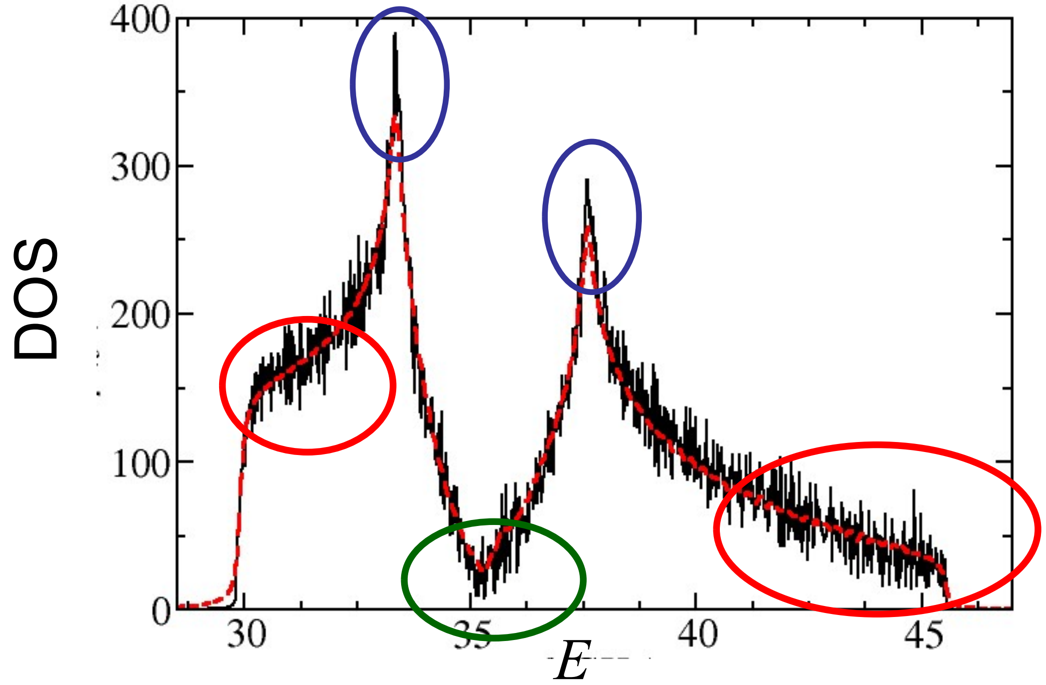

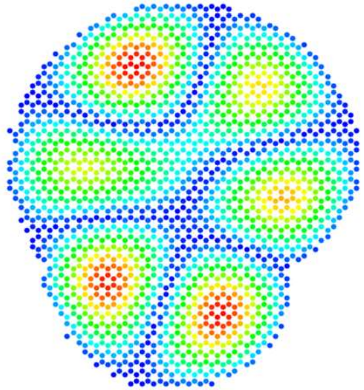

- Close to the band edges, GBs are described by the non-relativistic Schrödinger equation of the corresponding QB
- Around the Dirac points GBs are described by the Dirac equation of massless fermions
- The van Hove singularities border the Schrödinger and the Dirac region

Spectral Properties of Graphene & Quantum Billiard around Lower Band Edge

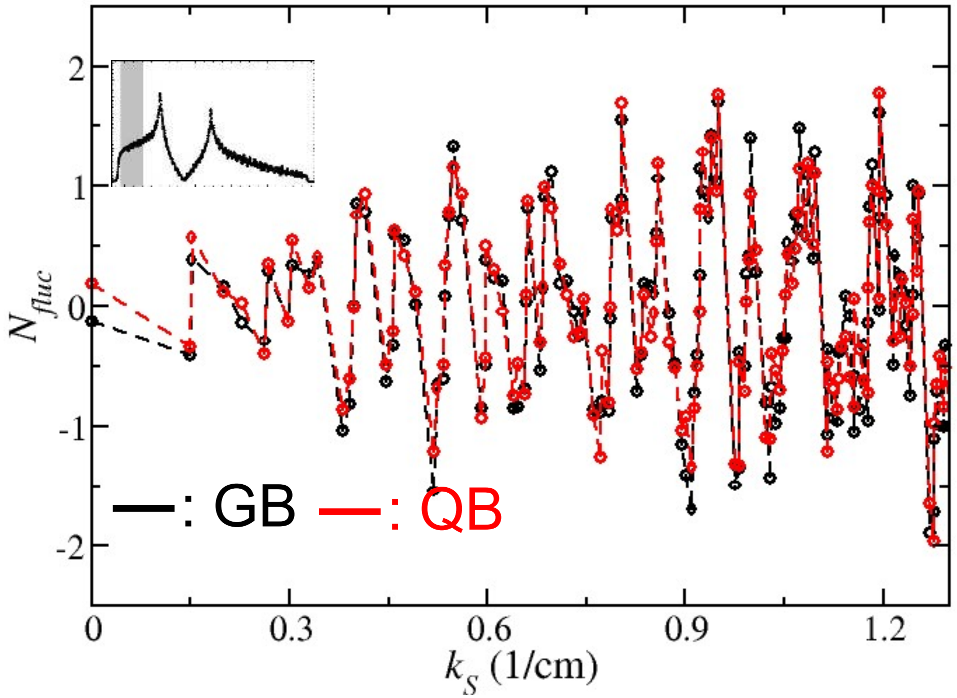

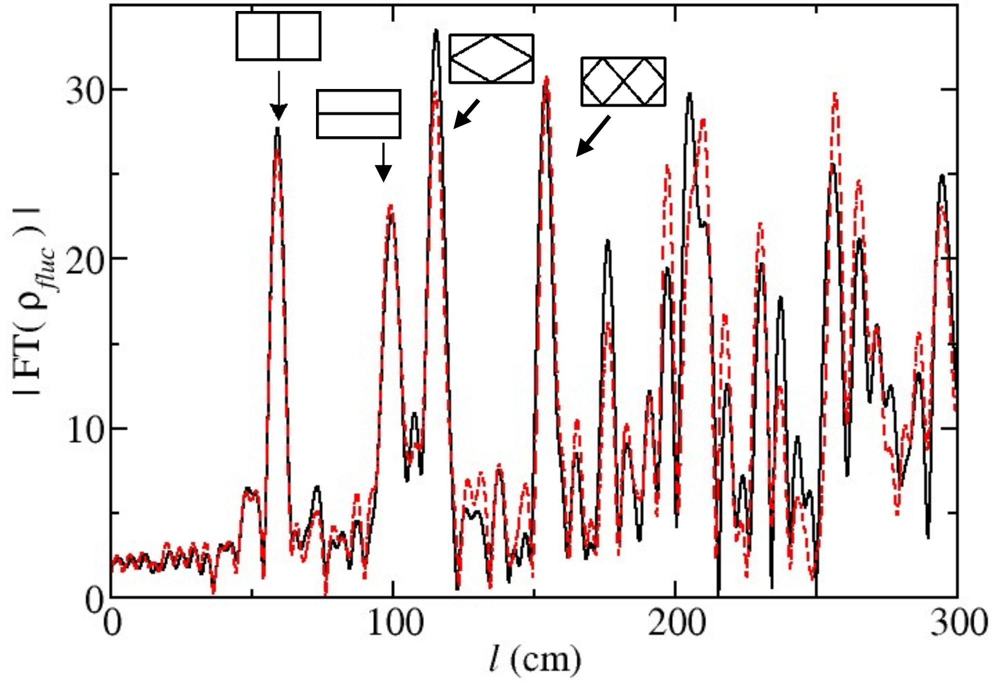

- Fluctuating part of integrated resonance density vs. eigenvalues k_s of QB

$$N_{fluc}(k) = N(k) - N_{smooth}(k)$$

- Length spectrum $|\tilde{\rho}(l)| = |\int_0^{k_{max}} \mathrm{d}k e^{ikl} \rho_{fluc}(k)|$

- Very good agreement between GB and QB

Intensity and Momentum Distributions Around Dirac Frequency

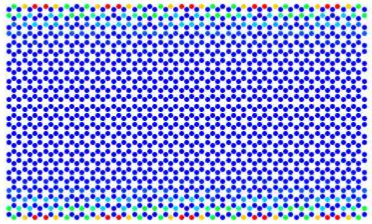

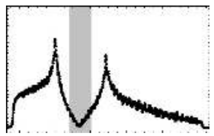

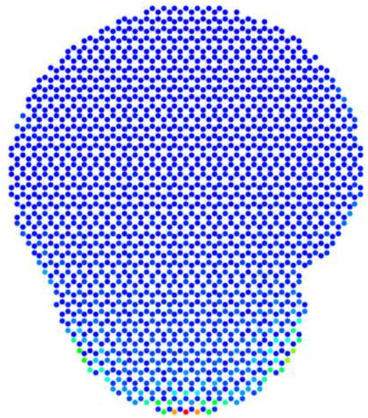

- Intensity is vanishing over the billiard area / localized at zigzag edges

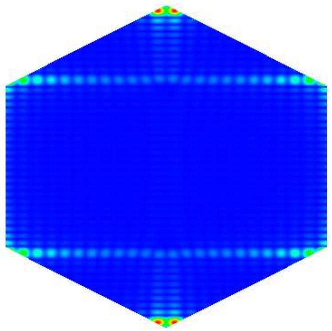

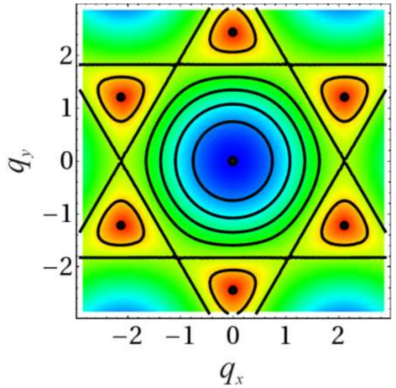

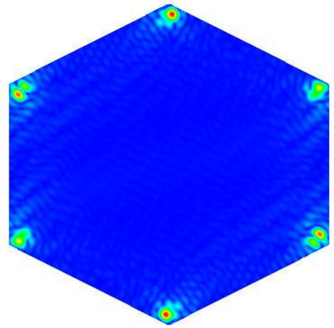

- Momentum distribution: Fourier transform of wave functions from (x,y) to (q_x,q_y)

$$\tilde{\psi}_n(q_x, q_y) = \iint_\Omega dx dy \psi_n(x, y) e^{-i\boldsymbol{q}\boldsymbol{r}}$$

- Momentum distributions are peaked at the $K_{\pm}$ points of the band structure

Spectral Properties Africa and Rectangular GBs

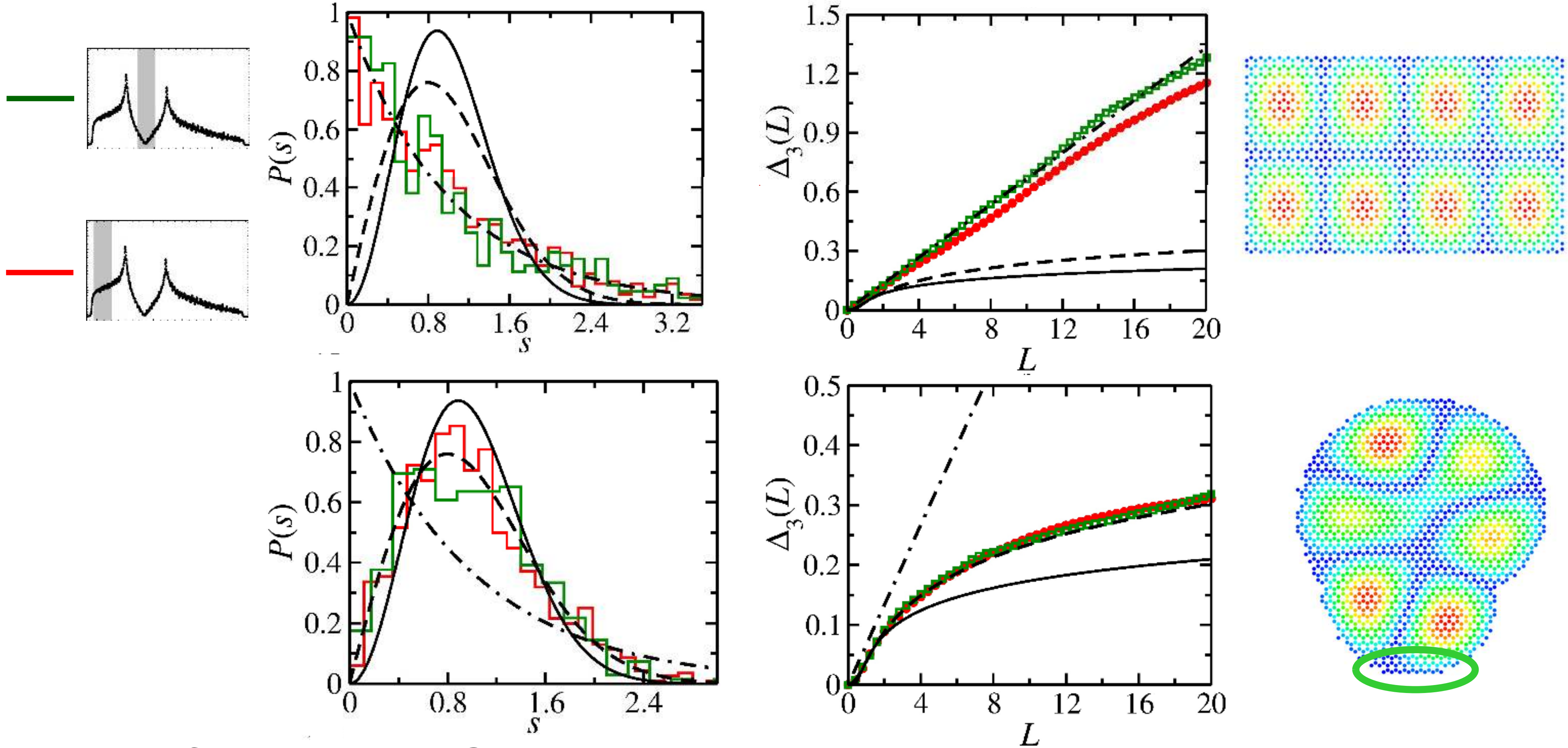

- In the Africa-shaped GB the nongeneric edge states had to be excluded
- Reason for deviations from GUE as in the NB: scattering at the boundaries induces mixing of the 2D Dirac equations

Distributions of Ratios of Nearest and Next-Nearest Eigenvalue Spacings

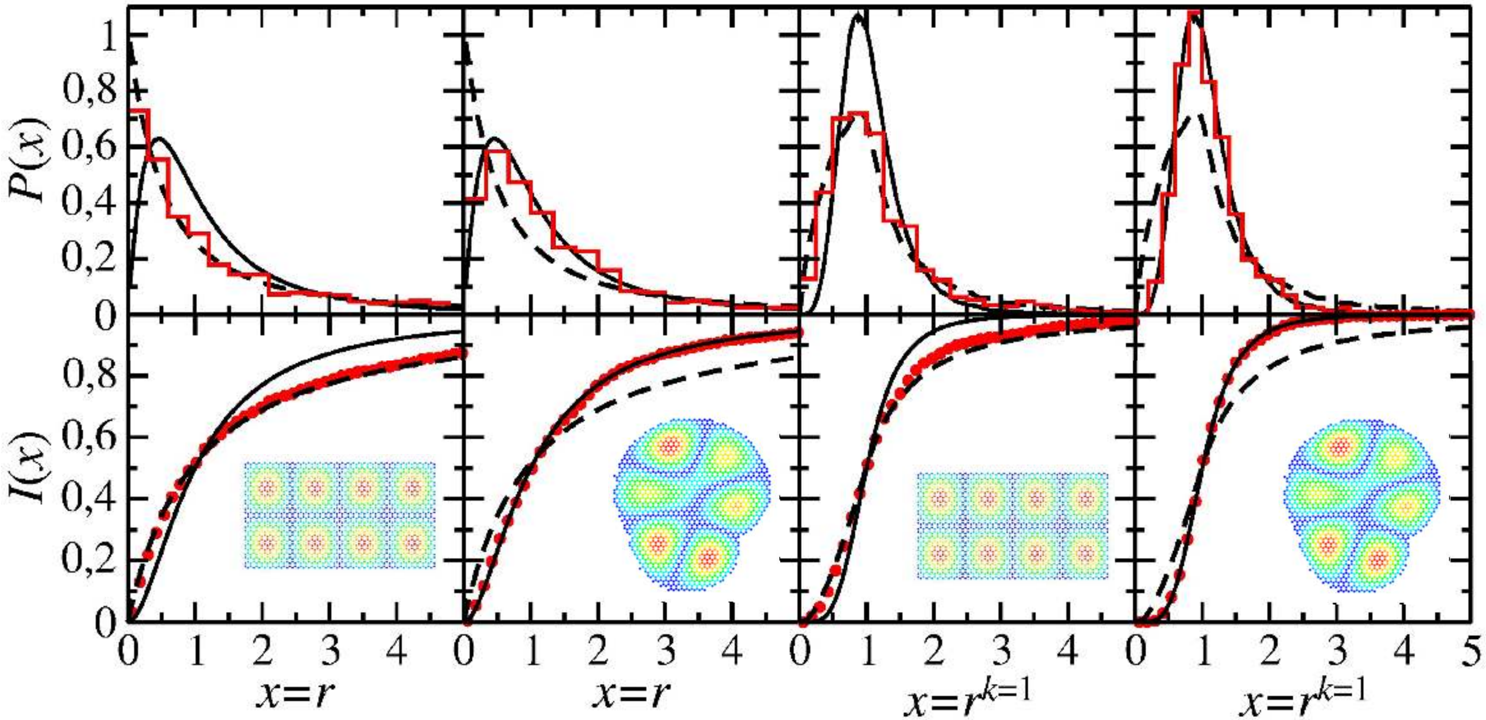

- At the van Hove singularity the DOS has a logarithmic singularity
  $\Rightarrow$ unfolding becomes cumbersome
- Compute ratio distributions using *all* eigenvalues

$\rightarrow$ Spectral properties of GB coincide with those of QB in all energy ranges

- Do the spectral properties of GBs only depend on its shape?

15° Circle Sector Graphene Billiard
[PRE94, 062214(2016)]

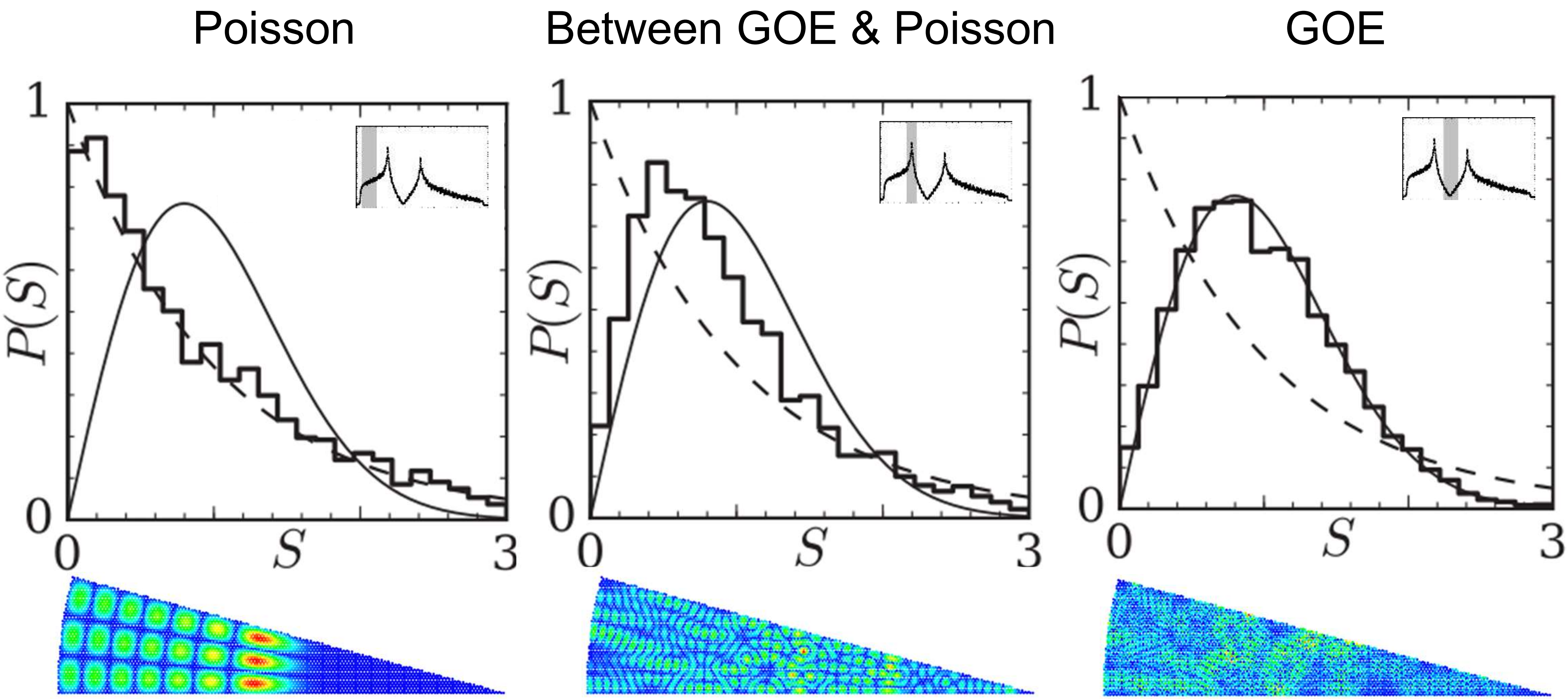

- With increasing energy the lattice structure starts to prevail leading to the occurrence of the van Hove singularities in the spectral density and the Dirac point → Spectral Properties of relativistic quantum billiards?

Spectral Properties of Massive Half-Circle NB

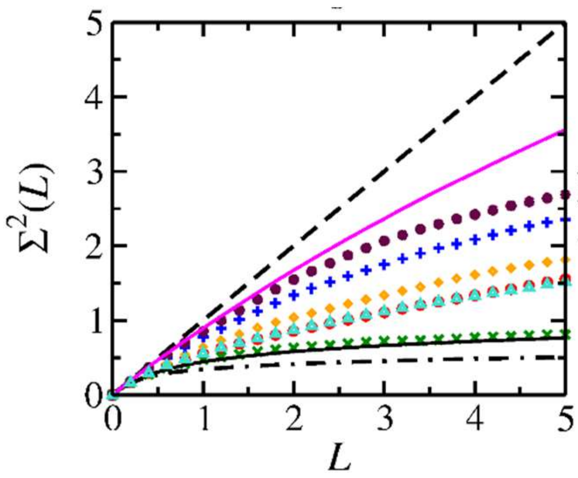

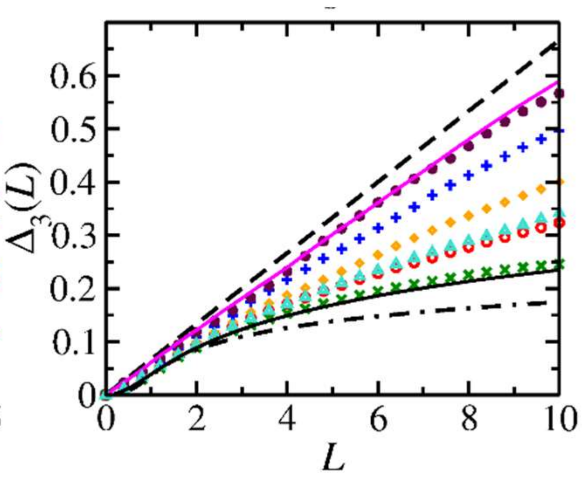

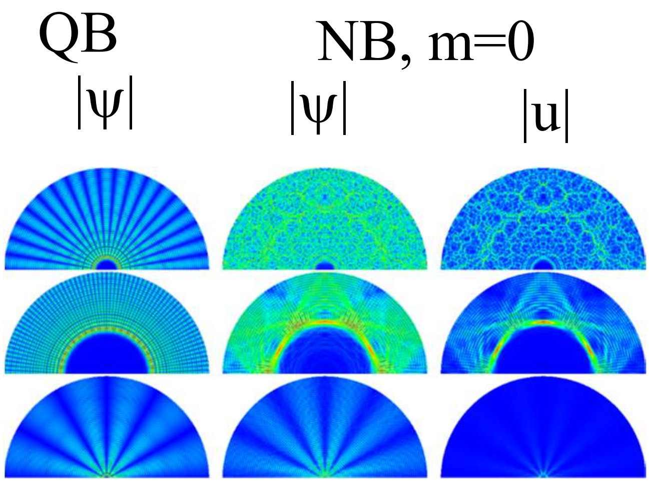

- Spectral properties of the QB agree with Poisson
- Spectral properties of the NB: m=0 (m=0), 10, 20, 50, 100 → QB
- Contributions of diameter orbit are extracted by employing its trace formula
- Spectral properties are close to GOE for m=0 and to that of the QB for m≥100

Billiards with a M-fold Rotational Symmetry

- Boundary with M-fold rotational symmetry: $w\left(\varphi+\lambda\frac{2\pi}{M}\right)=e^{i\lambda\frac{2\pi}{M}}w(\varphi)$
- Rotation operator in terms of angular momentum operator: $\hat{R}=e^{i\frac{2\pi}{M}\hat{L}}$
- Symmetry-projected eigenstates of the QB

$$\hat{R}^{\lambda}\psi_m^{(l)}(r,\varphi)=\psi_m^{(l)}\left(r,\varphi-\frac{2\pi}{M}\lambda\right)=e^{il\frac{2\pi}{M}\lambda}\psi_m^{(l)}(r,\varphi)\quad \lambda,\ l=0,1,2,\ldots,M-1$$

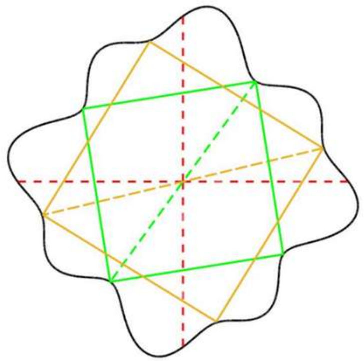

- Apply time-reversal operator:

$$\hat{C}\psi_m^{(l)}\left(r,\varphi-\frac{2\pi}{M}\lambda\right)=e^{-il\frac{2\pi}{M}\lambda}\left[\psi_m^{(l)}(r,\varphi)\right]^*=e^{i(M-l)\frac{2\pi}{M}\lambda}\left[\psi_m^{(l)}(r,\varphi)\right]^*$$

- States with $l=0,\ M/2$ are real. T-invariance implies that $l,\ M-l$ are degenerate doublets
- The spinor eigenfunctions of the NB may be separated into symmetry-projected eigenstates but components belong to different symmetry classes

$$\hat{R}\psi_{1,m}(\boldsymbol{r})=e^{il\frac{2\pi}{M}}\psi_{1,m}(\boldsymbol{r})$$
$$\hat{R}\psi_{2,m}(\boldsymbol{r})=e^{i(l-1)\frac{2\pi}{M}}\psi_{2,m}(\boldsymbol{r})$$

Graphene Billiards with 3fold Symmetry

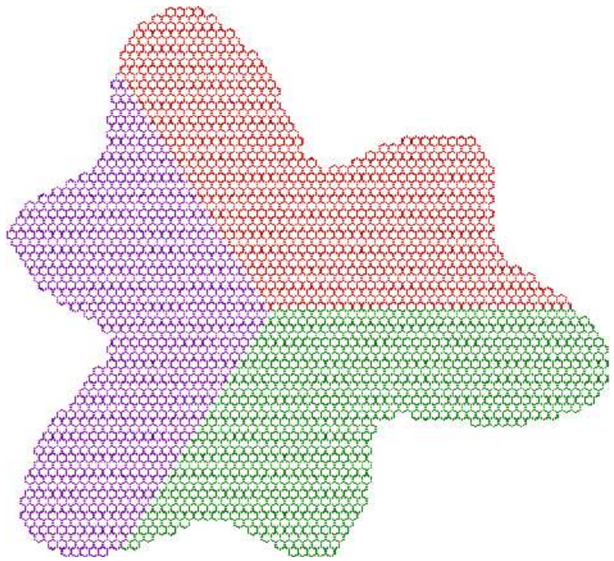

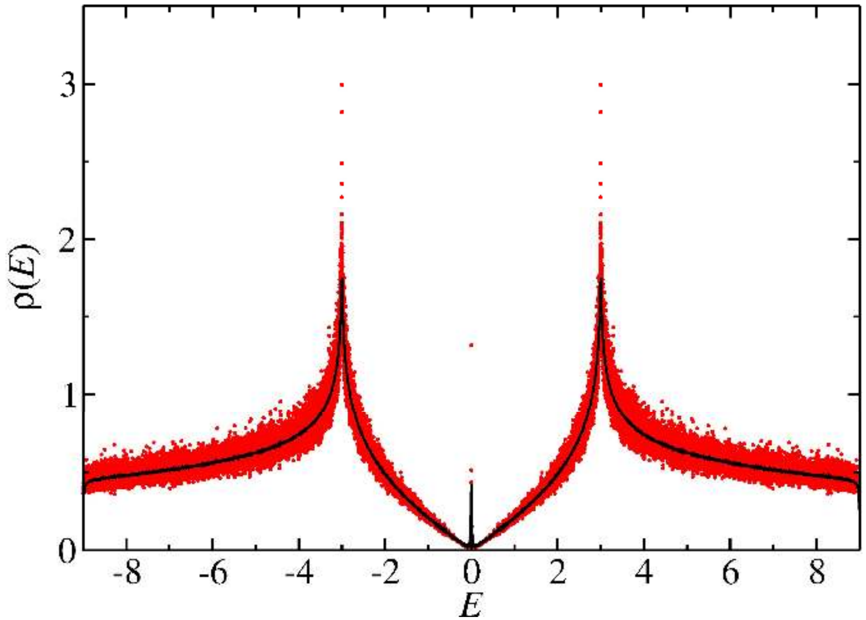

$$\hat{\mathcal{H}}_{TBM} = \begin{pmatrix} \hat{H} & \hat{V} & \hat{V}^T \\ \hat{V}^T & \hat{H} & \hat{V} \\ \hat{V} & \hat{V}^T & \hat{H} \end{pmatrix} \rightarrow \hat{U}^\dagger \hat{\mathcal{H}}_{TB} \hat{U} = \begin{pmatrix} \hat{H}^{TB(0)} & 0_N & \hat{0}_N \\ \hat{0}_N & \hat{H}^{TB(1)} & \hat{0}_N \\ \hat{0}_N & \hat{0}_N & \hat{H}^{TB(2)} \end{pmatrix} \rightarrow \begin{array}{l} \hat{H}^{TB(0)} = \hat{H} + \hat{V} + \hat{V}^T \\ \hat{H}^{TB(1)} = \hat{H} + e^{i\frac{2\pi}{3}}\hat{V} + e^{i\frac{4\pi}{3}}\hat{V}^T \\ \hat{H}^{TB(2)} = \hat{H} + e^{i\frac{4\pi}{3}}\hat{V} + e^{i\frac{2\pi}{3}}\hat{V}^T \end{array}$$

- $\hat{H}^{TB(0)}$ is real and $\hat{H}^{TB(1)}$, $\hat{H}^{TB(2)}$ are complex conjugate to each other with same eigenvalues
- The DOSs of complete spectrum, singlets and doublets are similar

Intensity Distributions for GB around Lower Band Edge & Quantum Billiard

GB

l=0

l=1

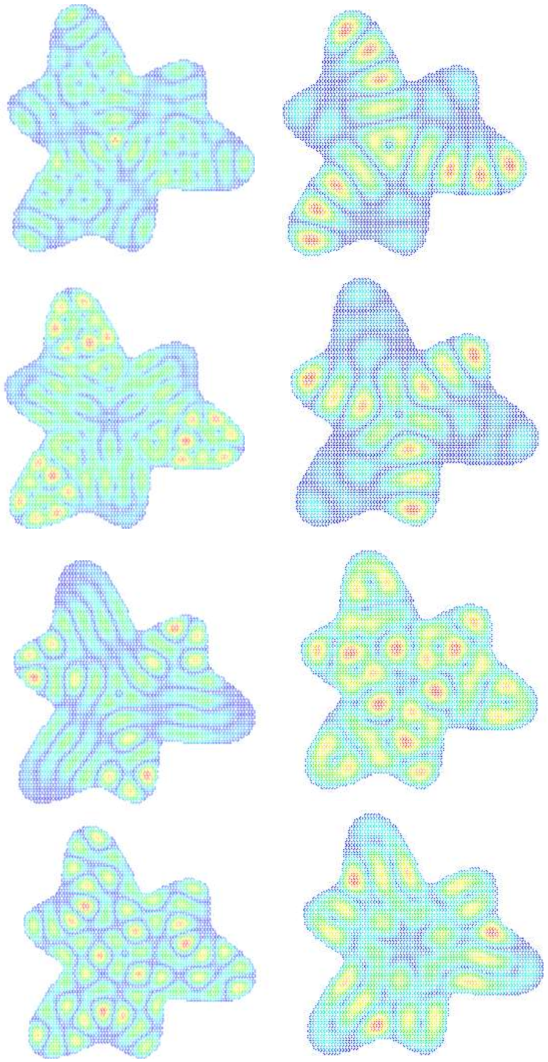

QB

l=0

l=1

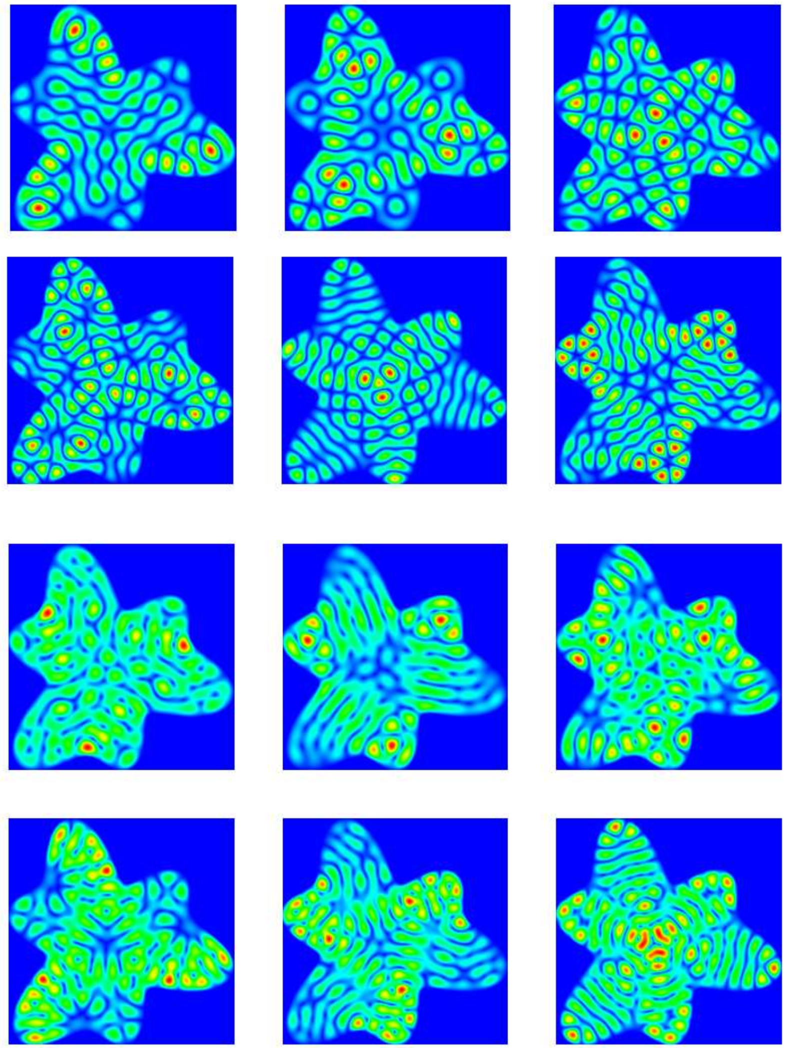

- Analogy between the eigenstates of the GB and QB holds up to n=150

Wave Functions and Momentum Distributions of the Graphene Billiard at the Dirac Point

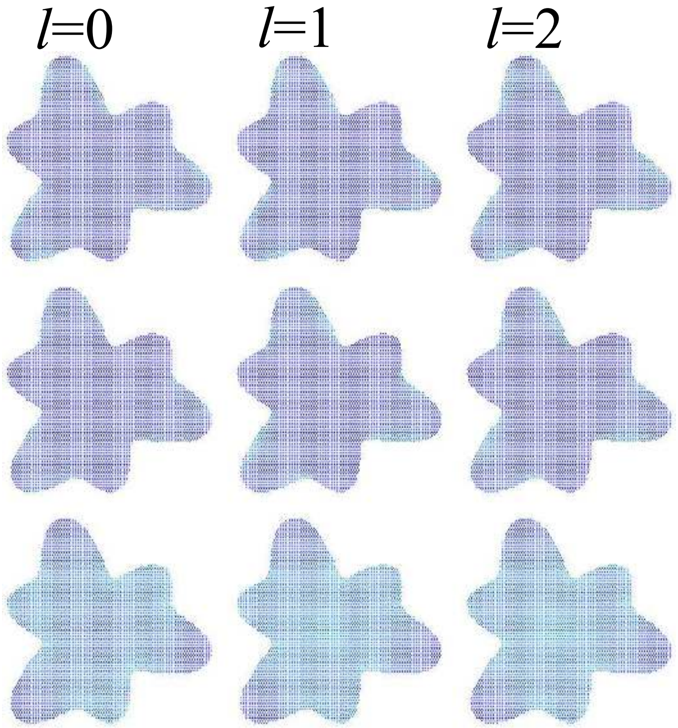

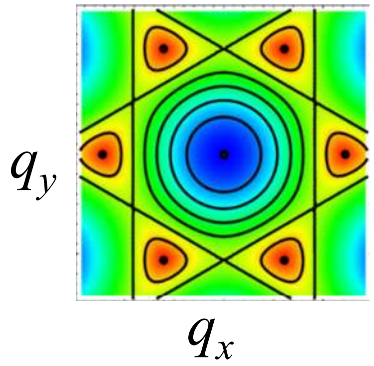

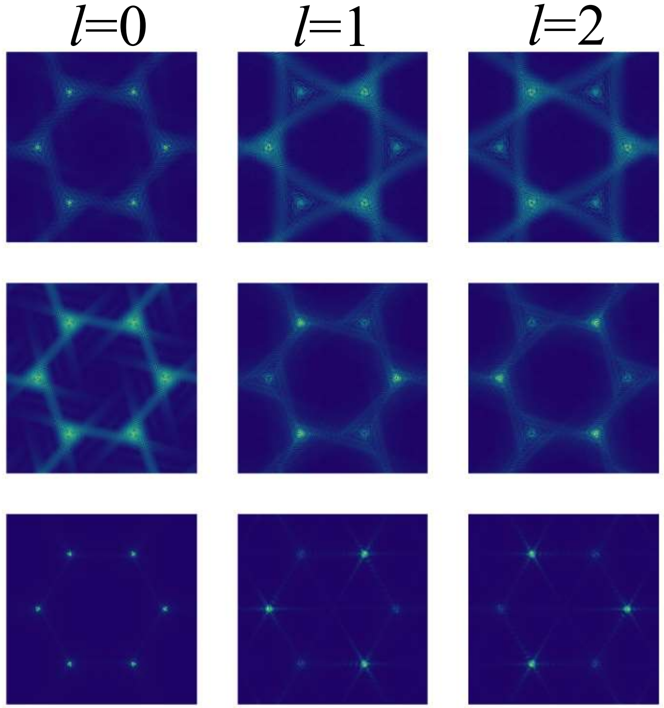

- For *l=1,2* the valley states at the K_+ & K_- points are excited selectively depending on *l* $\Rightarrow$ no intervalley scattering at boundary!
- Note: Spectral properties of GBs coincide with those of QBs because of valley mixing

Intensity Distributions for GB around the Dirac Point & Neutrino Billiard

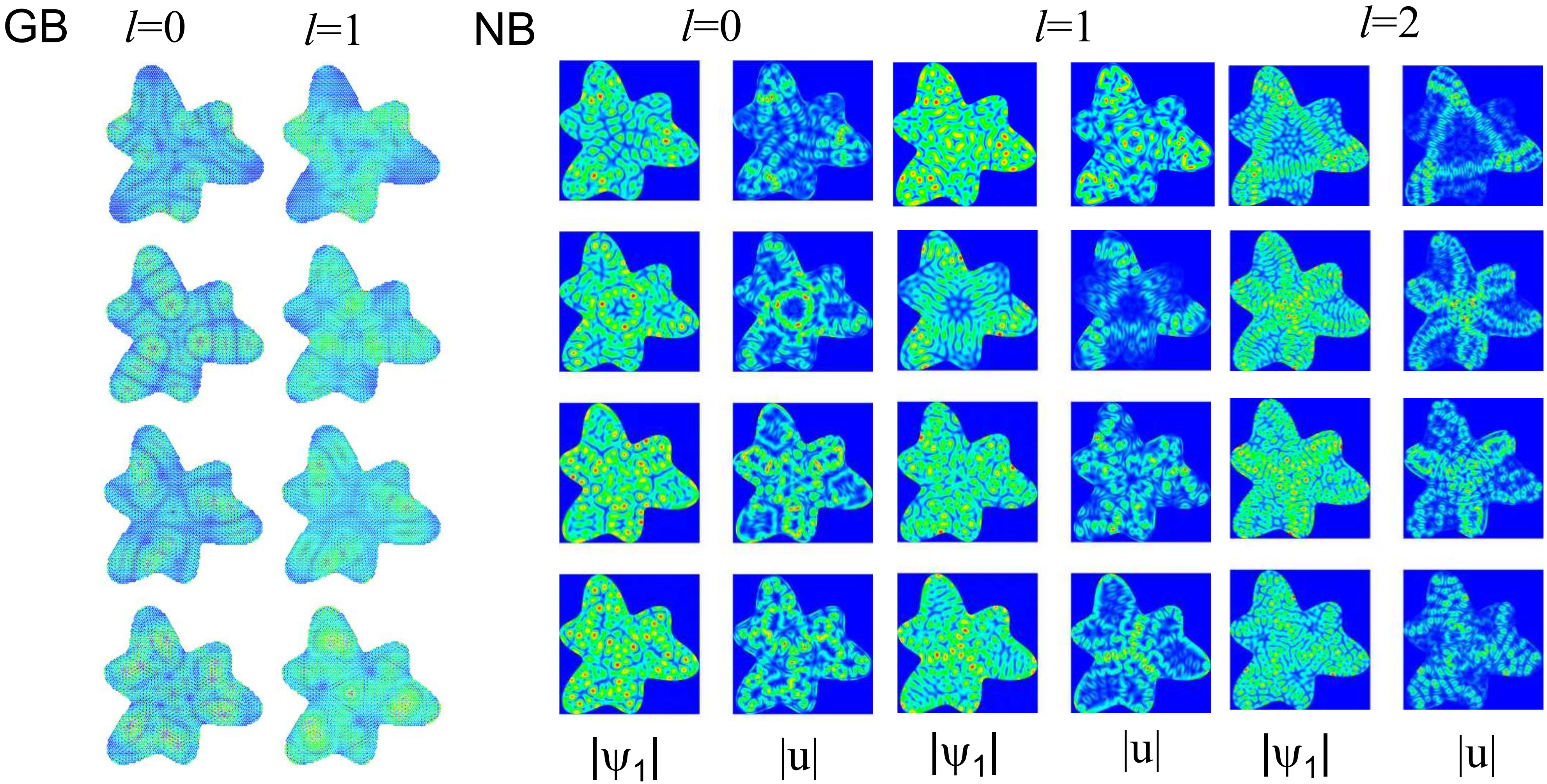

- Local current: $\hat{\boldsymbol{u}} = \boldsymbol{\nabla}_{\boldsymbol{p}} \hat{H}_D = c\hat{\boldsymbol{\sigma}},\ \boldsymbol{u}(\boldsymbol{r}) = c\psi^\dagger \hat{\boldsymbol{\sigma}} \psi$

Spectral Properties of the C_3 GB, QB & NB

- GB:

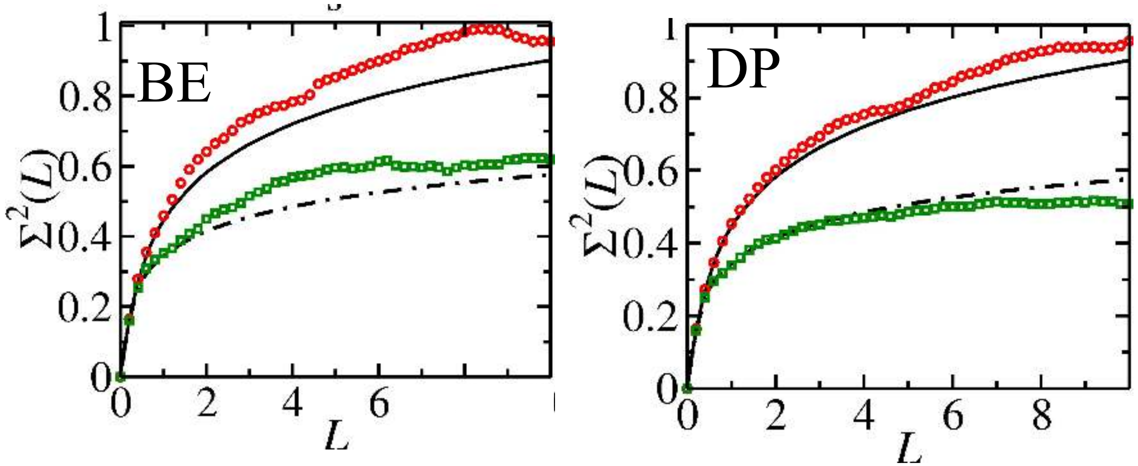

— : Singlets

— : Doublets

QB & NB

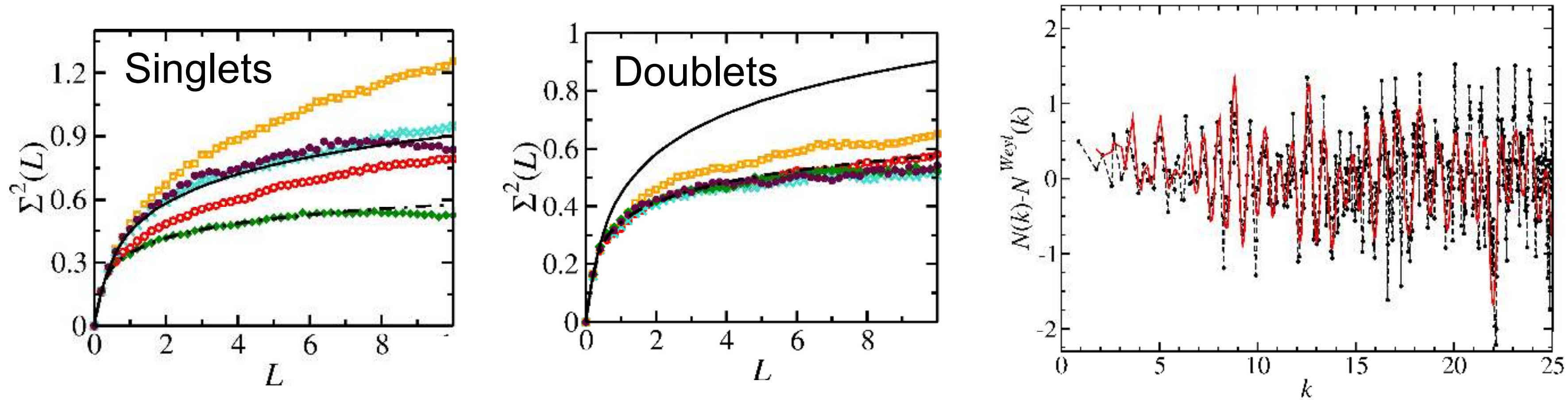

- Spectral properties for mass m=0, m=50, m=100 (100), and for the QB
- Non-generic orbits manifest themselves as slow oscillations in $N^{fluc}(k)$

$\rightarrow$ After extraction agreement with RMT predictions is good

Spectral Properties of the C_3 GB, NB & QB

Graphene Billiard

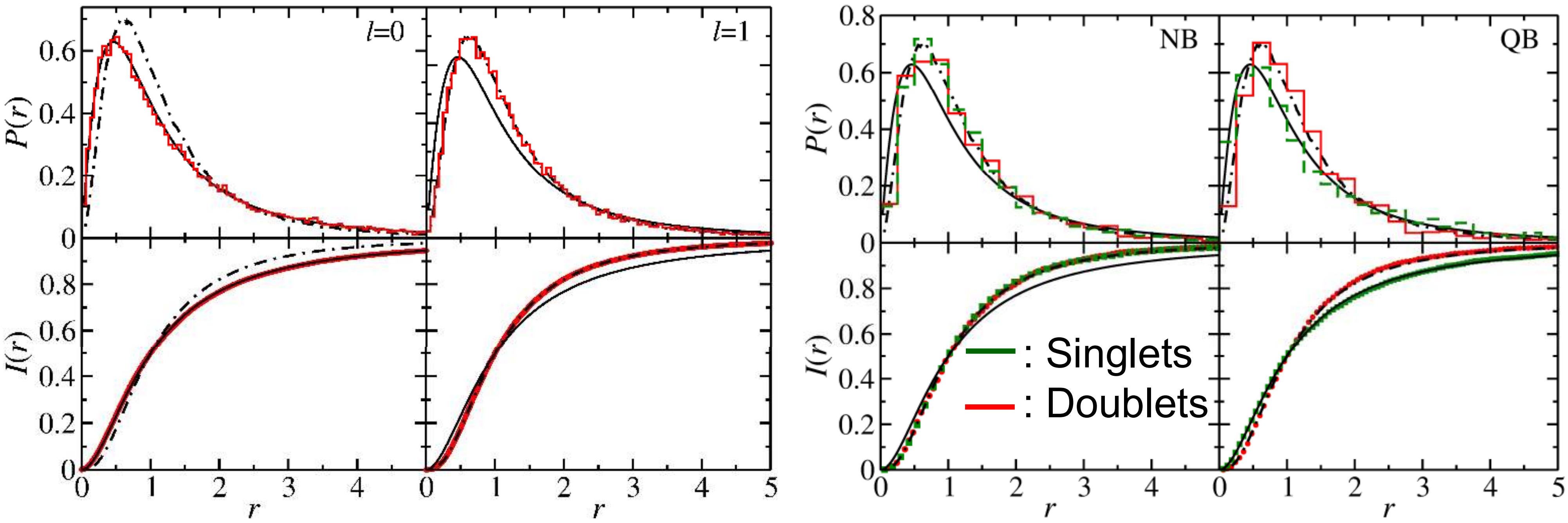

- GB & QB: spectral properties of the singlets (doublets) coincide with GOE (GUE) statistics
- For the NB the spectral properties of the singlets and doublets coincide with GUE

Graphene Billiards with 4fold Symmetry

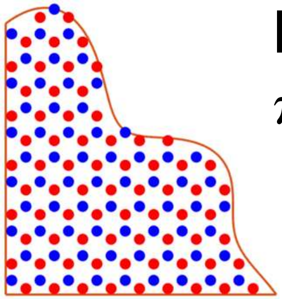

Rotate by $\pi/2$

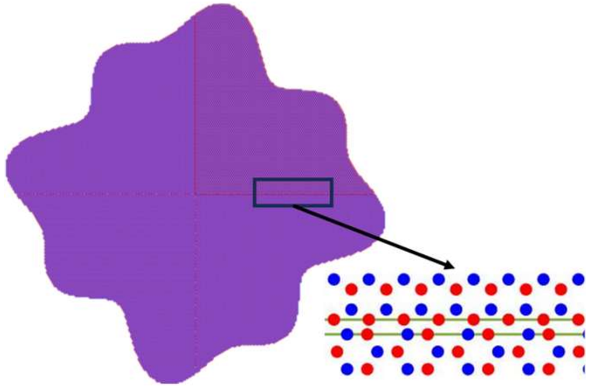

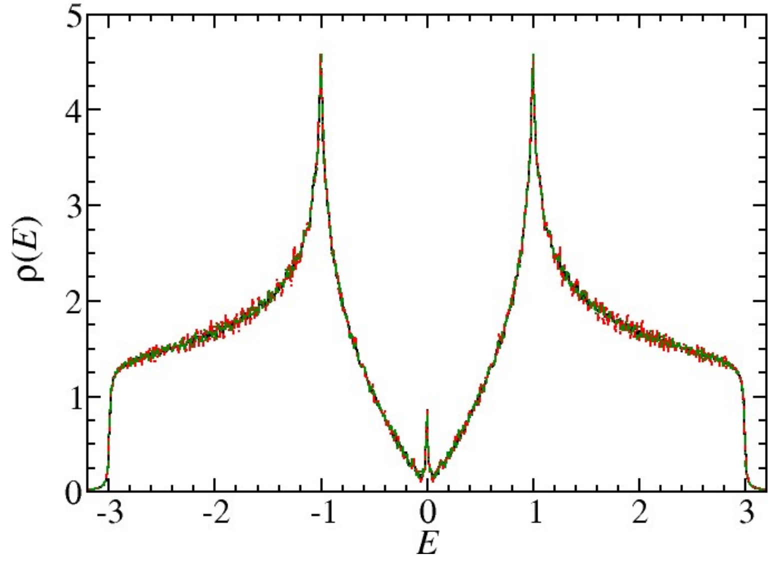

$$\hat{\mathcal{H}}_{ij}^{TB} = t_0\delta_{ij} + t_{1;ij}\tilde{\delta}(|\boldsymbol{r}_i - \boldsymbol{r}_j| - d_{ij})$$

$$\hat{\mathcal{H}}^{TB} = \begin{pmatrix} \hat{H} & \hat{V} & 0 & \hat{V}^T \\ \hat{V}^T & \hat{H} & \hat{V} & 0 \\ 0 & \hat{V}^T & \hat{H} & \hat{V} \\ \hat{V} & 0 & \hat{V}^T & \hat{H} \end{pmatrix} \rightarrow \hat{U}^\dagger \hat{\mathcal{H}}^{TB} \hat{U} = \begin{pmatrix} \hat{H}^{TB(0)} & 0_N & \hat{0}_N & \hat{0}_N \\ \hat{0}_N & \hat{H}^{TB(1)} & \hat{0}_N & \hat{0}_N \\ \hat{0}_N & \hat{0}_N & \hat{H}^{TB(2)} & \hat{0}_N \\ \hat{0}_N & \hat{0}_N & \hat{0}_N & \hat{H}^{TB(3)} \end{pmatrix} \rightarrow$$

$$\hat{H}^{TB(0)} = \hat{H} + \left[\hat{V} + \hat{V}^T\right]$$
$$\hat{H}^{TB(2)} = \hat{H} - \left[\hat{V} + \hat{V}^T\right]$$
$$\hat{H}^{TB(1)} = \hat{H} - i\left[\hat{V} - \hat{V}^T\right]$$
$$\hat{H}^{TB(3)} = \hat{H} + i\left[\hat{V} - \hat{V}^T\right]$$

- $\hat{H}^{TB(0)}$ & $\hat{H}^{TB(2)}$ are real and $\hat{H}^{TB(1)}$ & $\hat{H}^{TB(3)}$ are complex conjugate to each other with same eigenvalues
- The DOSs of complete spectrum, singlets and doublets are similar

Center for Theoretical Physics of Complex Systems

Wave Functions and Momentum Distributions of the C_4 Graphene Billiard

Lower Band Edge

Van Hove Singularities

Dirac Point

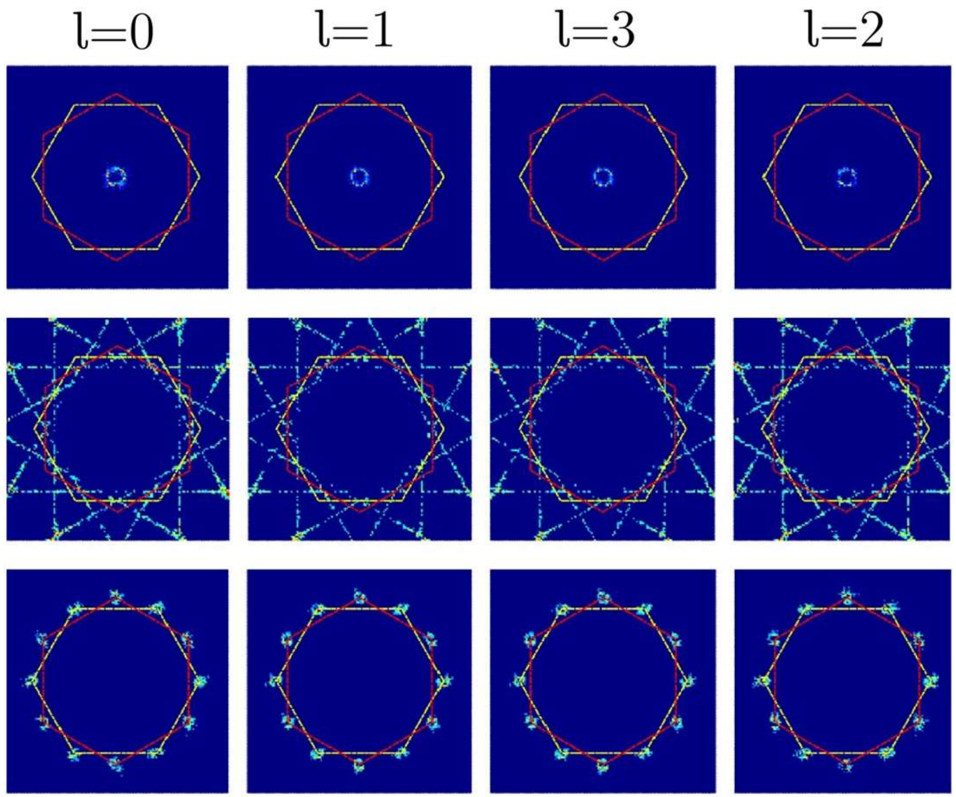

- The band structure of propating modes exhibits 12 saddle points and 12 Dirac points

Spectral Properties of the C_4 QB, NB & GB

QB

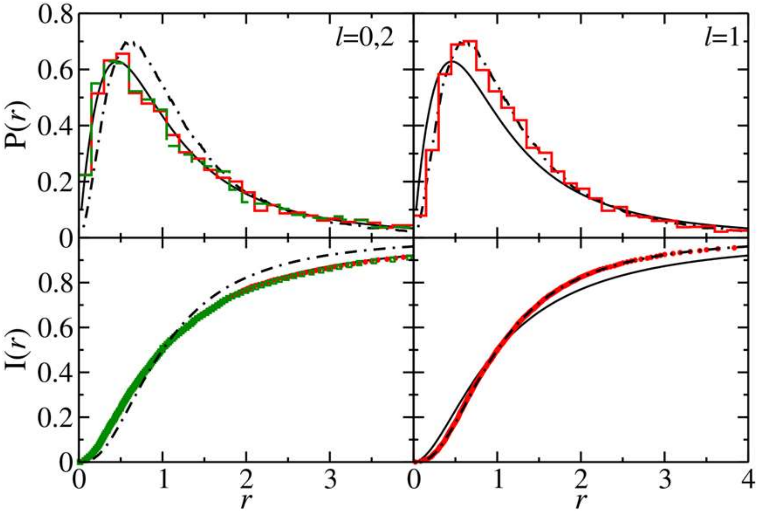

NB

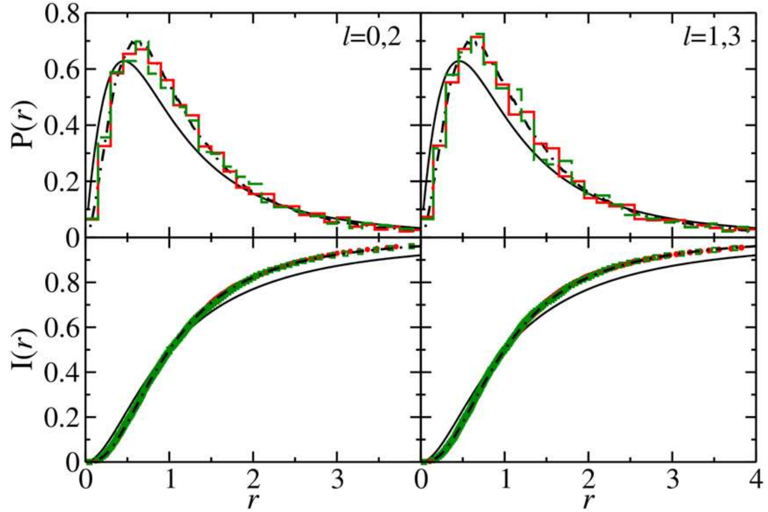

GB

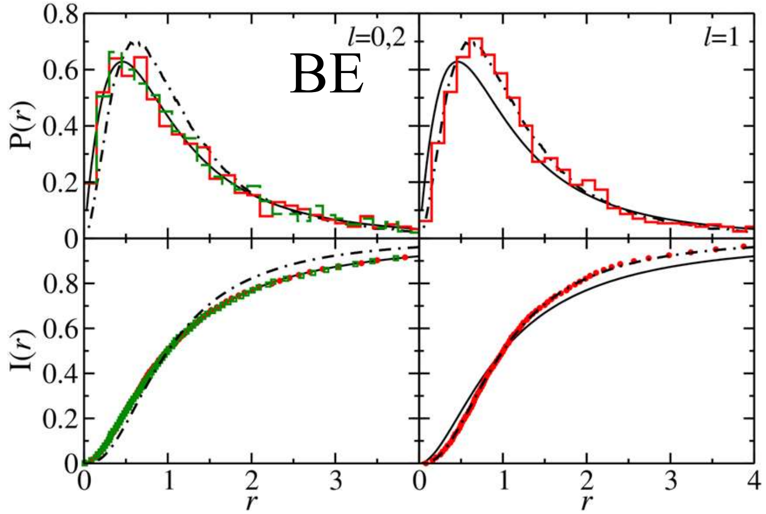

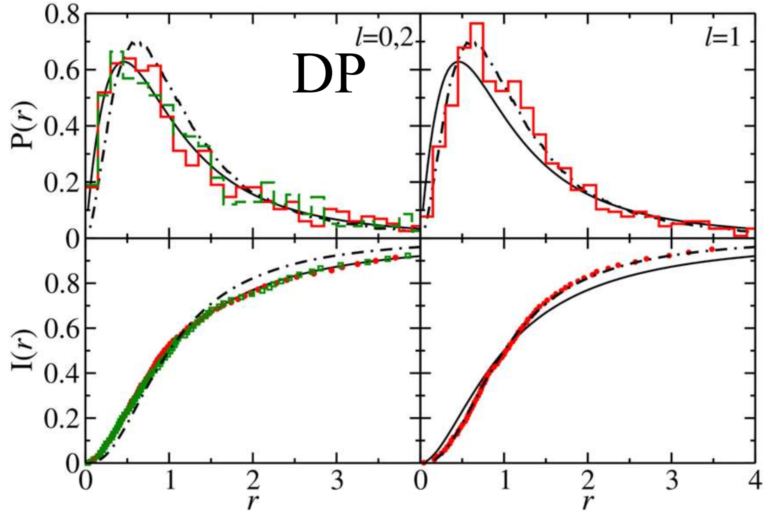

- Spectral properties of GB agree with those of QB

Quantum Billiards and Microwave Billiards

- Experimental determination of the eigenvalues and wave functions of quantum billiards with microwave billiards

Quantum billiard

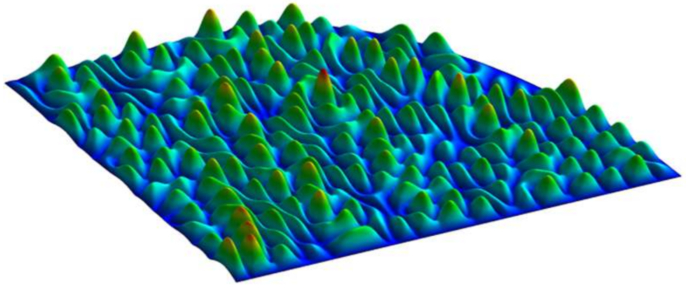

Microwave billiard

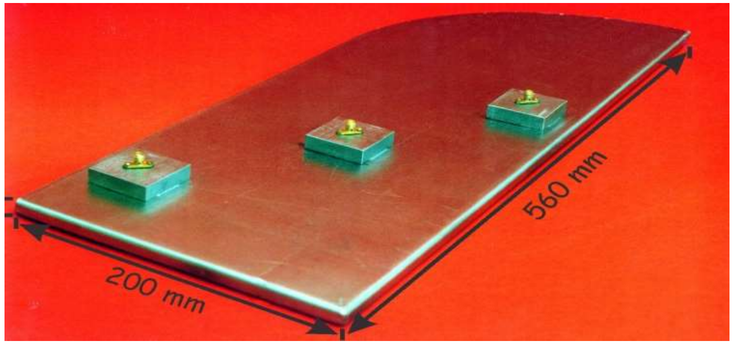

$$\longleftrightarrow$$

$$f < f_{max} = c/2h$$

$$k = \frac{2\pi f}{c}$$

$$\left(\frac{\hbar^2}{2m}\Delta + E\right)\Psi = 0, \quad \Psi\big|_{\partial\Omega} = 0$$

$$\left(\Delta + k^2\right) E_z = 0, \quad E_z\big|_{\partial\Omega} = 0$$

eigenvalue E $\leftrightarrow$ resonance frequency f

eigenfunction Ψ $\leftrightarrow$ electric field strength E_z

Superconducting Dirac Billiards

BD et al., PRB 91, 035411 (2015), PRL 116, 023901 (2016)

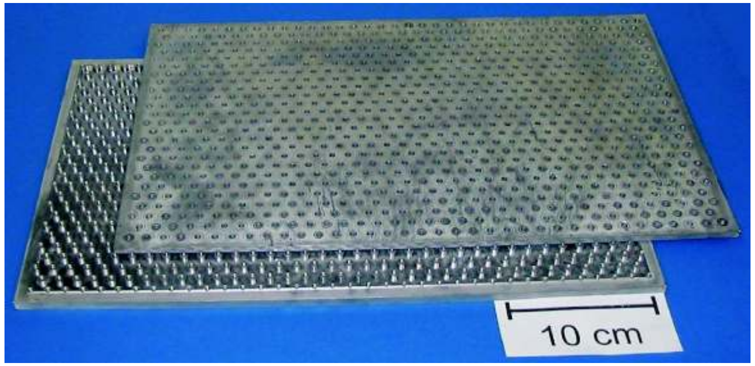

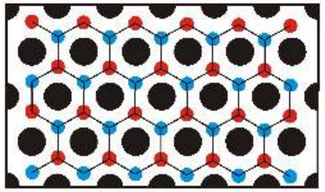

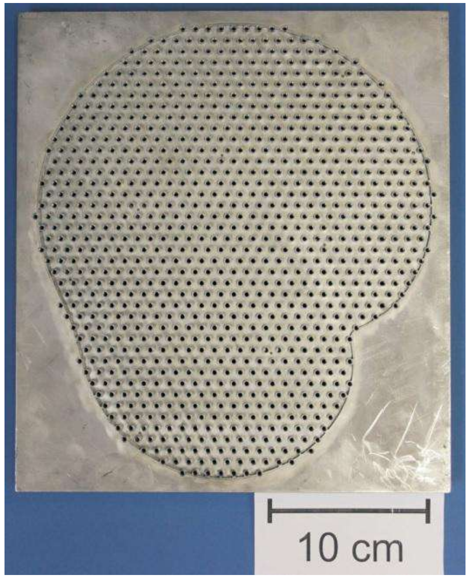

- For the photonic crystal ~ 900 cylinders are milled out of a brass plate
- Basin and lid are covered with lead
- Lead is superconducting below T_c=7.2 K $\rightarrow$ high Q value at T_{LHe}=4 K
- Height h = 3 mm $\rightarrow$ 2D system for $f < c/2h$ = 50 GHz

Center for Theoretical Physics of Complex Systems

Density of States (DOS) of the Complete Measured Spectrum

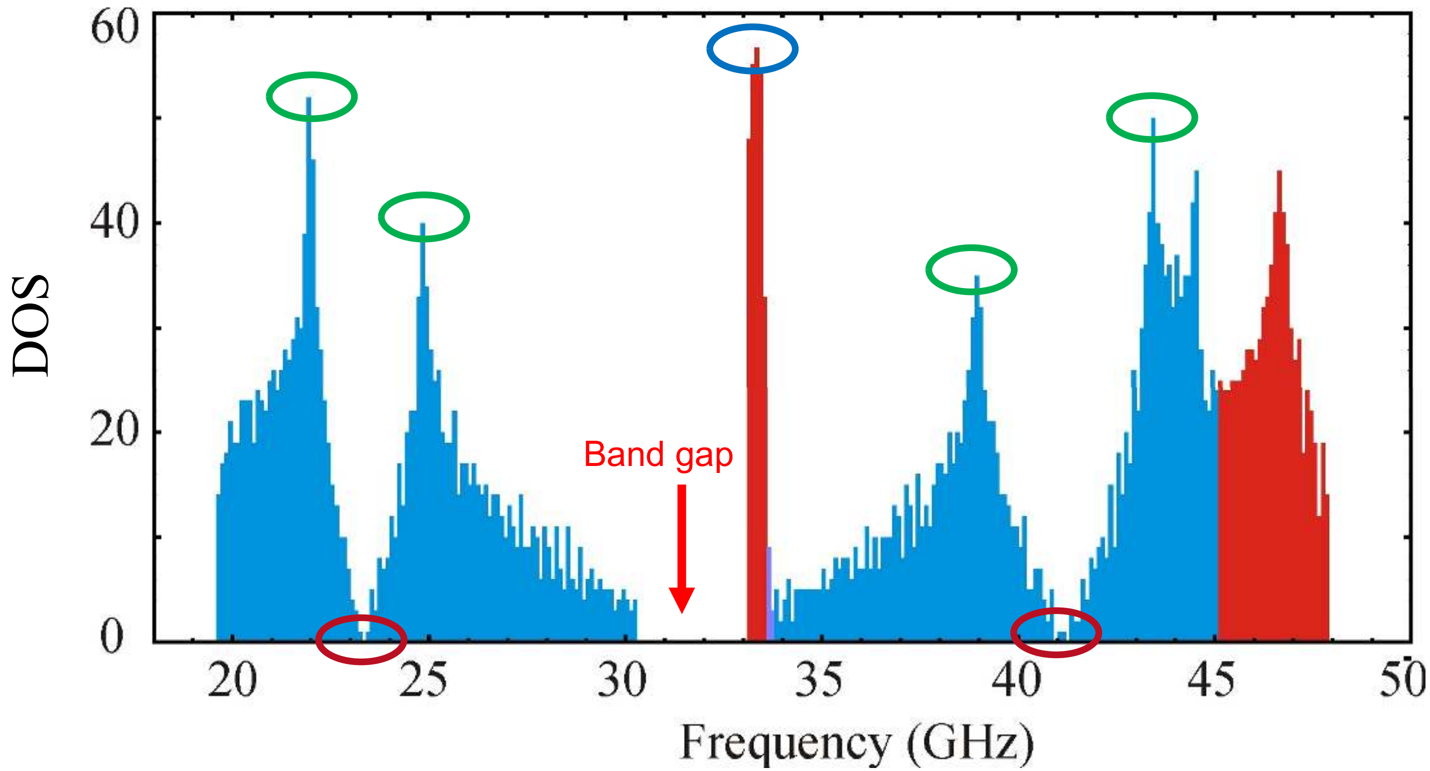

- The DOS exhibits two Dirac points framed by van Hove singularities that are separated by a band gap and a nearly flat band
- Occurrence of the flat band cannot be explained with a honeycomb-based tight-binding model

Electric-Field Intensity Distributions Below, Inside & Above the FB

- Below FB:

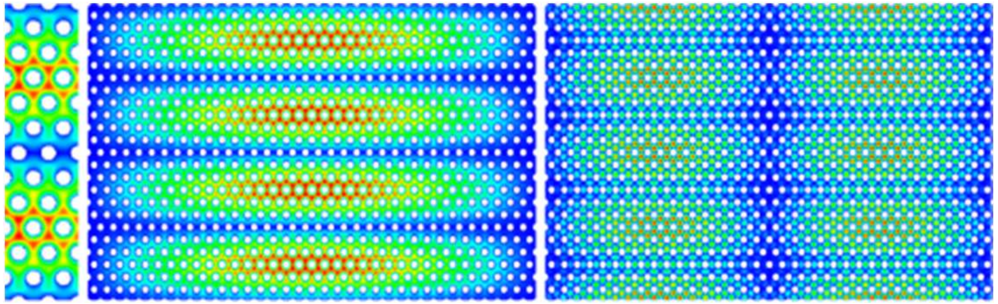

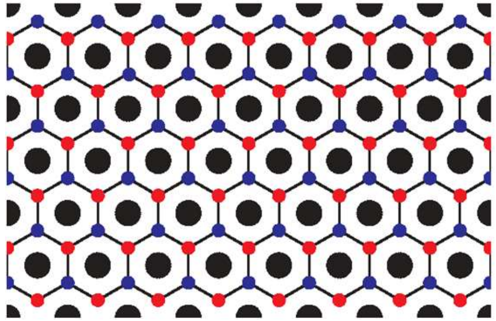

- At FB:

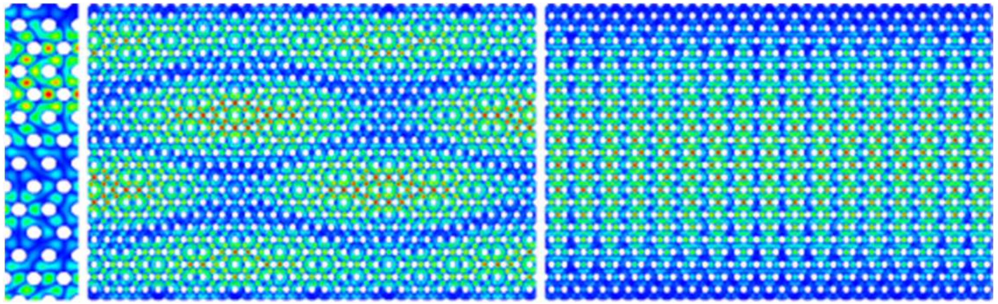

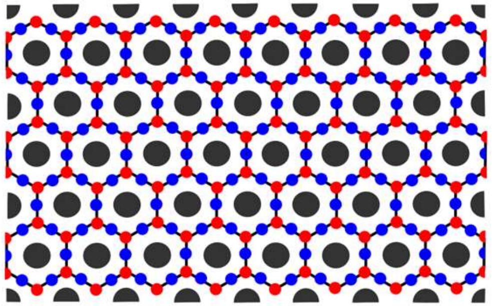

- Above FB:

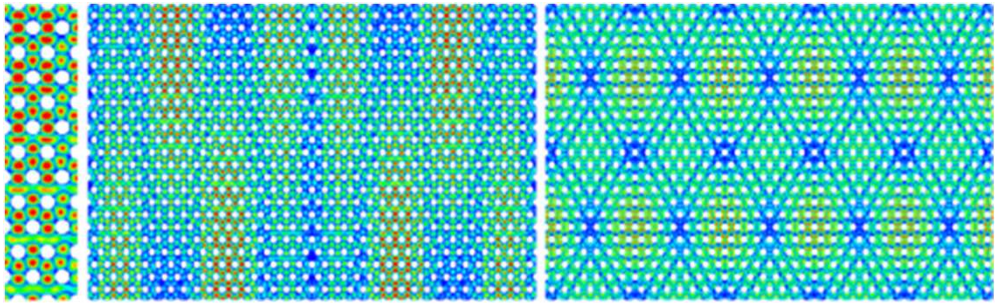

Wolfgang Akkermann, TEMF, TU-Darmstadt

Fit of TBM for Honeycomb-Kagome Lattice to Experimental DOS

[W. Maimaiti et al., PRB102, 214301 (2020)]

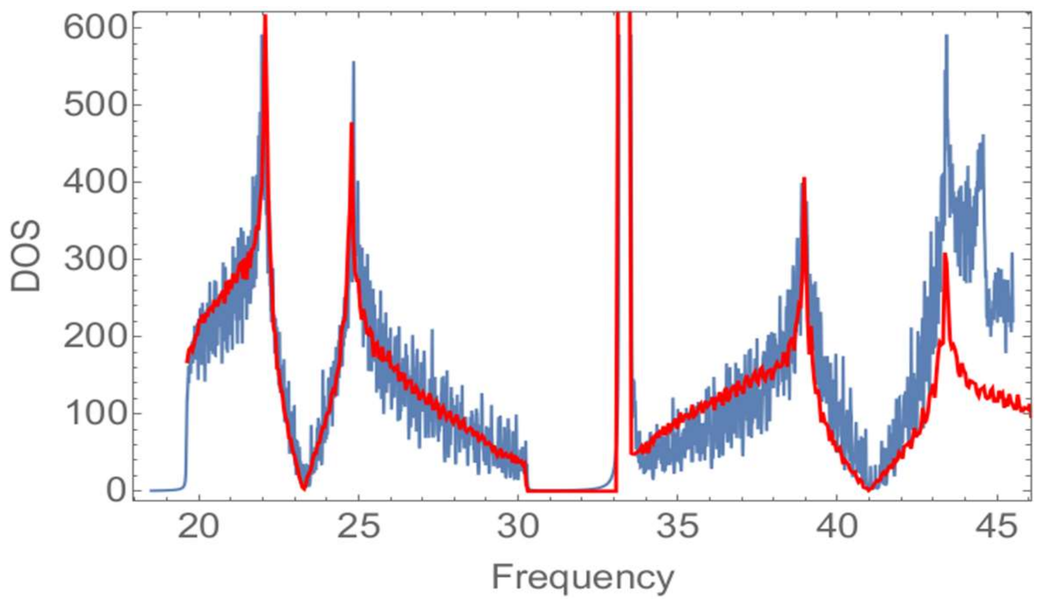

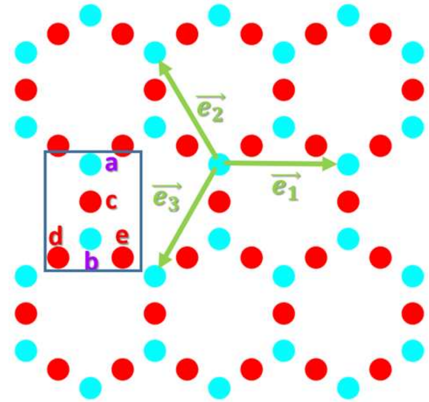

- Lattice = combination of honeycomb and kagome sublattices
- Tight-binding Hamiltonian

$$\hat{\mathcal{H}}_{ij}^{TBM} = t_0\delta_{ij} + t_1\delta(|\boldsymbol{r}_i - \boldsymbol{r}_j| - d_0) + t_2\hat{\delta}(|\boldsymbol{r}_i - \boldsymbol{r}_j| - d_1) + \ldots..$$

- Spectral properties and electric-field distributions are well described by the honome-based TBM with up to 6th n.n. hopping

Intensity Distributions of Honome & Dirac Billiard

[Weihua Zhang & BD, PRB 104, 064310 (2021)]

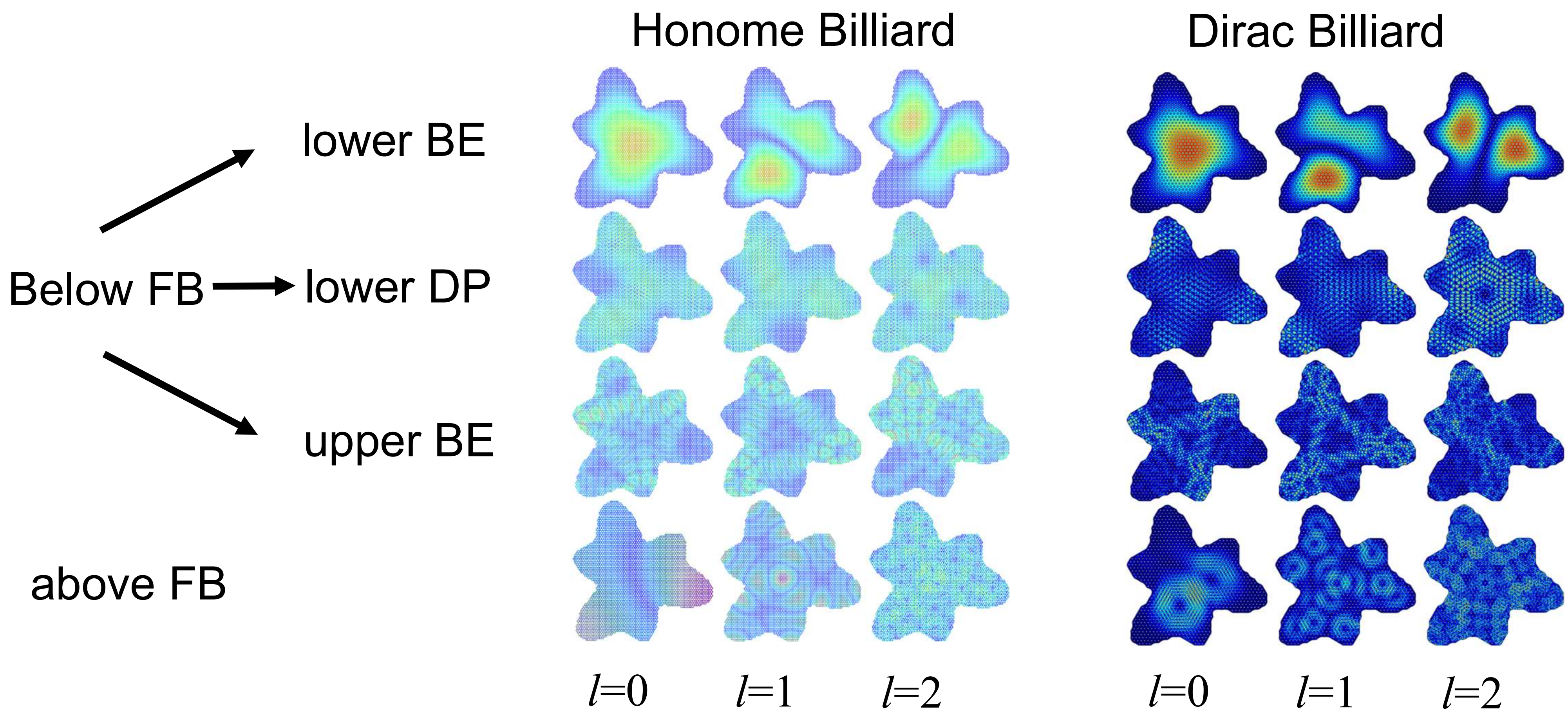

- The electric-field distributions of the microwave photonic crystal are well reproduced by the HB

Ratio & k=1 Overlapping Ratio Distributions of *all* eigenvalues of the Dirac & Honome Billiard

Dirac Billiard

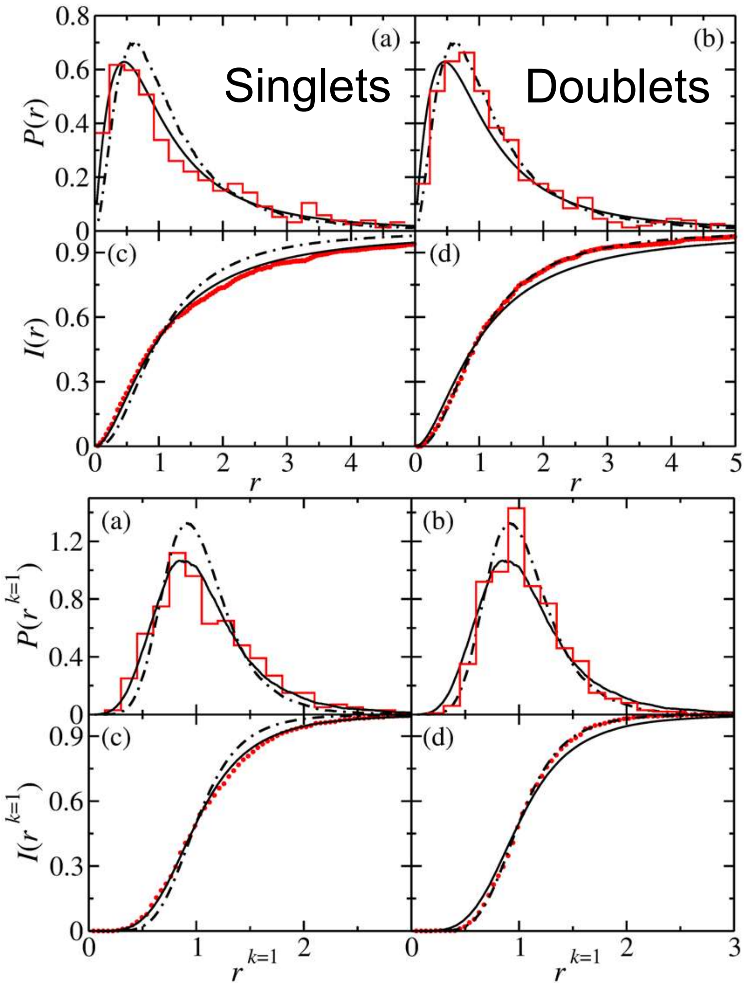

Honome Billiard

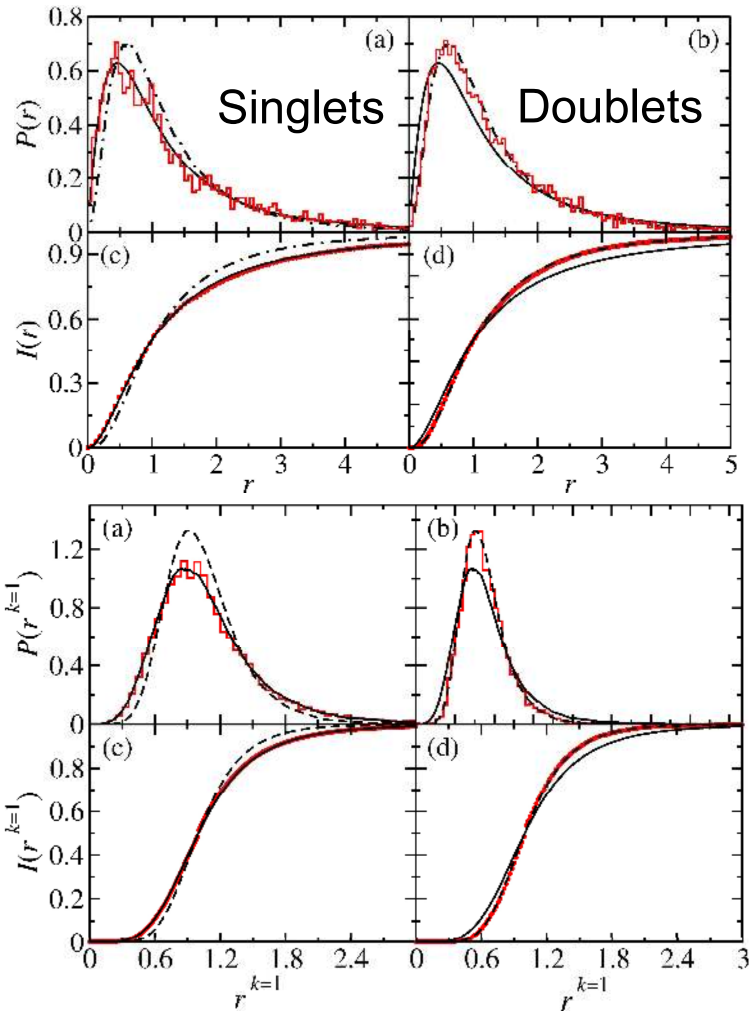

Thank you

for

your attention

Transmission Spectrum of Rectangular Dirac Billiard at 4 K

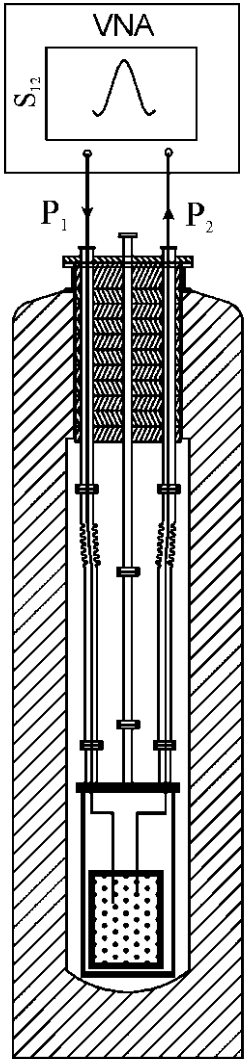

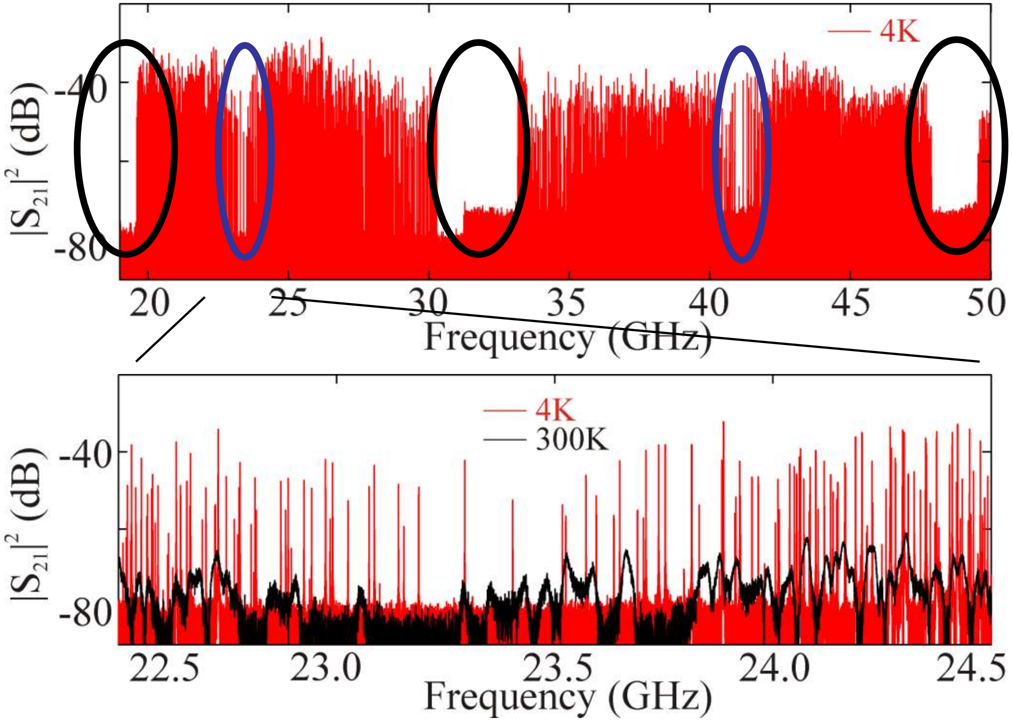

- Measured S-matrix: $|S_{21}|^2 = P_2 / P_1$
- Quality factors $> 5 \cdot 10^5$
- Pronounced band gaps and Dirac points
- Extracted ~5000 resonance frequencies (eigenvalues)

Measurement Principle

- Measurement of the scattering matrix element S_{21}

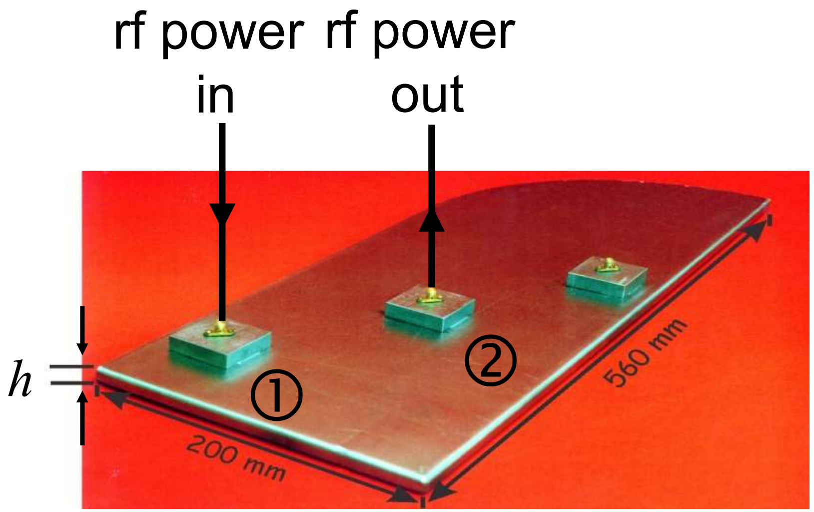

$$\longrightarrow \quad \frac{P_{out,2}}{P_{in,1}} = \left|S_{21}\right|^2$$

Resonance spectrum

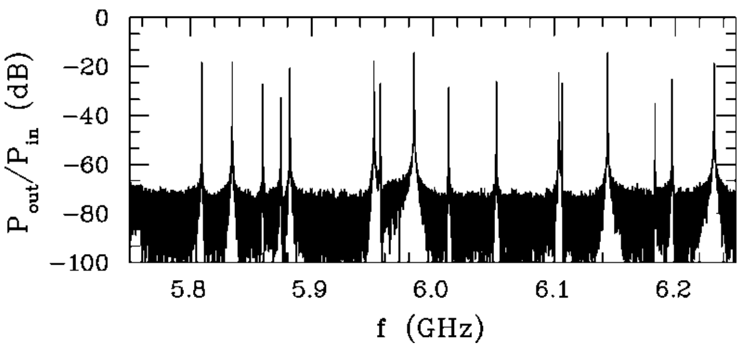

$\longrightarrow$ positions of the resonances $f_n = k_n c/2\pi$ yield eigenvalues

Graphene & Honome Billiards with 3fold Symmetry

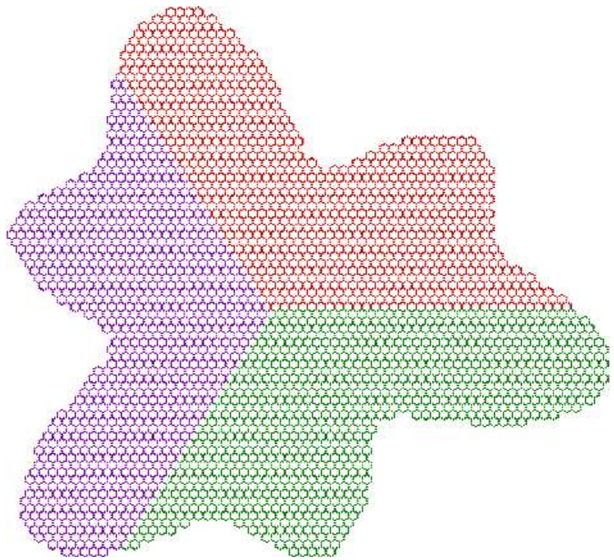

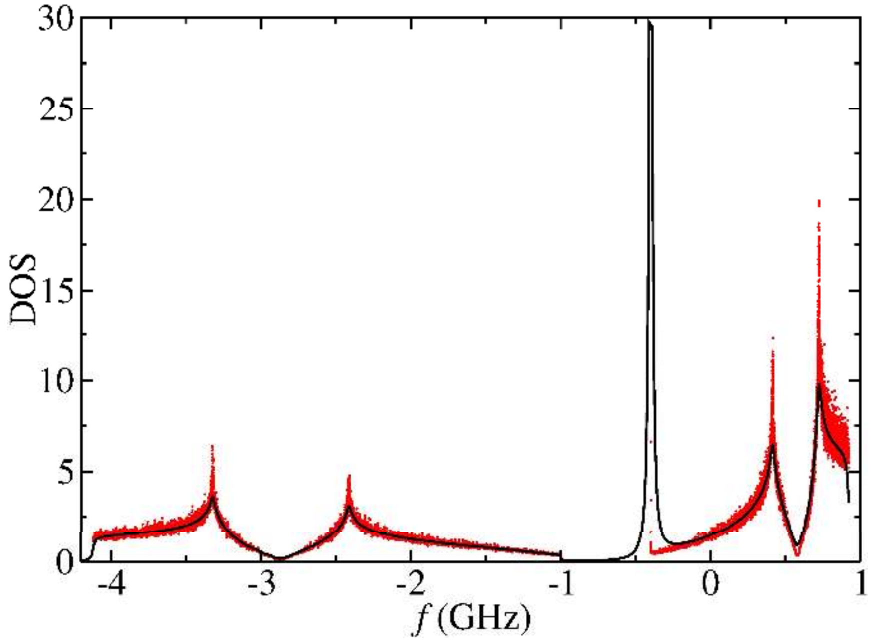

$$\hat{\mathcal{H}}_{TBM} = \begin{pmatrix} \hat{H} & \hat{V} & \hat{V}^T \\ \hat{V}^T & \hat{H} & \hat{V} \\ \hat{V} & \hat{V}^T & \hat{H} \end{pmatrix} \rightarrow \hat{U}^\dagger \hat{\mathcal{H}}_{TB} \hat{U} = \begin{pmatrix} \hat{H}^{TB(0)} & 0_N & \hat{0}_N \\ \hat{0}_N & \hat{H}^{TB(1)} & \hat{0}_N \\ \hat{0}_N & \hat{0}_N & \hat{H}^{TB(2)} \end{pmatrix} \rightarrow \begin{array}{l} \hat{H}^{TB(0)} = \hat{H} + \hat{V} + \hat{V}^T \\ \hat{H}^{TB(1)} = \hat{H} + e^{i\frac{2\pi}{3}}\hat{V} + e^{i\frac{4\pi}{3}}\hat{V}^T \\ \hat{H}^{TB(2)} = \hat{H} + e^{i\frac{4\pi}{3}}\hat{V} + e^{i\frac{2\pi}{3}}\hat{V}^T \end{array}$$

- $\hat{H}^{TB(0)}$ is real and $\hat{H}^{TB(1)}$, $\hat{H}^{TB(2)}$ are complex conjugate to each other with same eigenvalues
- The DOSs of complete spectrum, singlets and doublets are similar

Center for Theoretical Physics of Complex Systems

Wave functions of the Massive Neutrino Billiard

1500 levels, $kr_0 \in [0,35]$

Singlets l=0 | Doublets l=1 | Doublets l=2

$|\psi_1|$ $|\psi_2|$ $|\psi_1|$ $|\psi_2|$ $|\psi_1|$ $|\psi_2|$

m=0

m=20

m=100

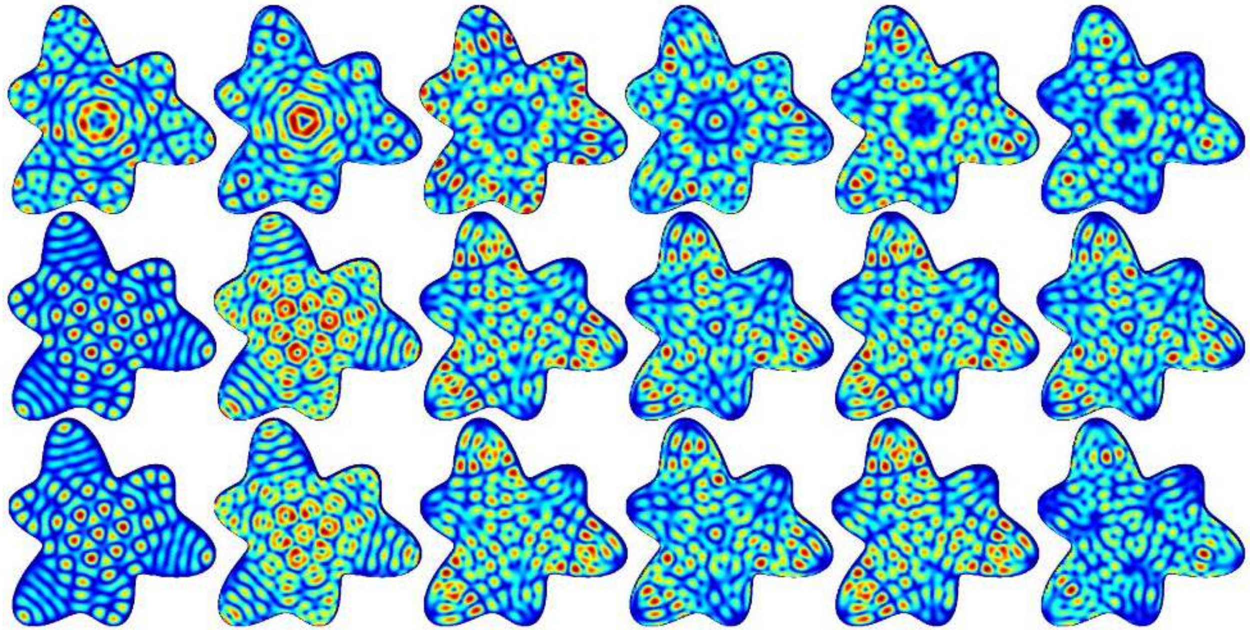

- For $m \to \infty$ the wave function components $\psi_{1,2}$ decouple and $|\psi_2 / \psi_1| \to 0$
- The nodal-line structure of the singlets becomes discernible because $\mathrm{Im}(\psi_{1,2}) \to 0$
- The intensity distributions of the doublets become similar
- The wave functions approach those of the QB

Unfolding of Spectra

- Integrated spectral density $N(E)$ = # levels below E
- Decompose into a smooth and a fluctuating part

$$N(E) = \overline{N}(E) + N^{fluc}(E)$$

- Replace eigenvalues E_i by the smooth part of the integrated spectral density

$$e_i = \overline{N}(E_i)$$

- Quantum billiard / Microwave billiard:

Weyl formula: $$\overline{N}\left(k = \sqrt{E}\right) = N^{Weyl}(k) = \frac{A}{4\pi}k^2 - \frac{U}{4\pi}k + const.$$

Dirac Equation for Massive Neutrino Billiards

- The energy E is given in terms of the free space wavevector k as

$$E = \hbar c k_E = \hbar c k\sqrt{1+\beta^2},\ \beta = \frac{mc}{\hbar k}$$

- The nonrelativistic limit $k\beta \to \infty$ complies with the BC
- Define

$$\psi = \begin{pmatrix} \sqrt{\frac{1+\sin\theta_\beta}{2}}\tilde{\psi}_1 \\ \sqrt{\frac{1-\sin\theta_\beta}{2}}\tilde{\psi}_2 \end{pmatrix} \qquad \sin\theta_\beta = \frac{\beta}{\sqrt{1+\beta^2}}.$$

nonrel. Limit $\Leftrightarrow$ $\theta_\beta \to \pi/2$
ultrarel. Limit $\Leftrightarrow$ $\theta_\beta \to 0$

$$\Rightarrow \quad k\tilde{\boldsymbol{\psi}}(\boldsymbol{r}) + i\hat{\boldsymbol{\sigma}}\cdot\nabla\tilde{\boldsymbol{\psi}}(\boldsymbol{r}) = 0$$ with $$\tilde{\psi}_2(s) = ie^{i\alpha(s)}\mathcal{K}^{-1}\tilde{\psi}_1(s) \qquad \mathcal{K} = \sqrt{\frac{1-\sin\theta_\beta}{1+\sin\theta_\beta}}$$

- The resulting Dirac equation has the same form as for massless neutrino billiards [Berry & Mondragon, Proc. R. Soc. London A **412**, 53 (1987)]
- Weyl formula: $$\overline{N}\left(k=\sqrt{E}\right) = N^{Weyl}(k) = \frac{A}{4\pi}k^2 \cancel{- \frac{U}{4\pi}k} + const.$$

Center for Theoretical Physics of Complex Systems

Experimental DOS and Topology of Band Structure

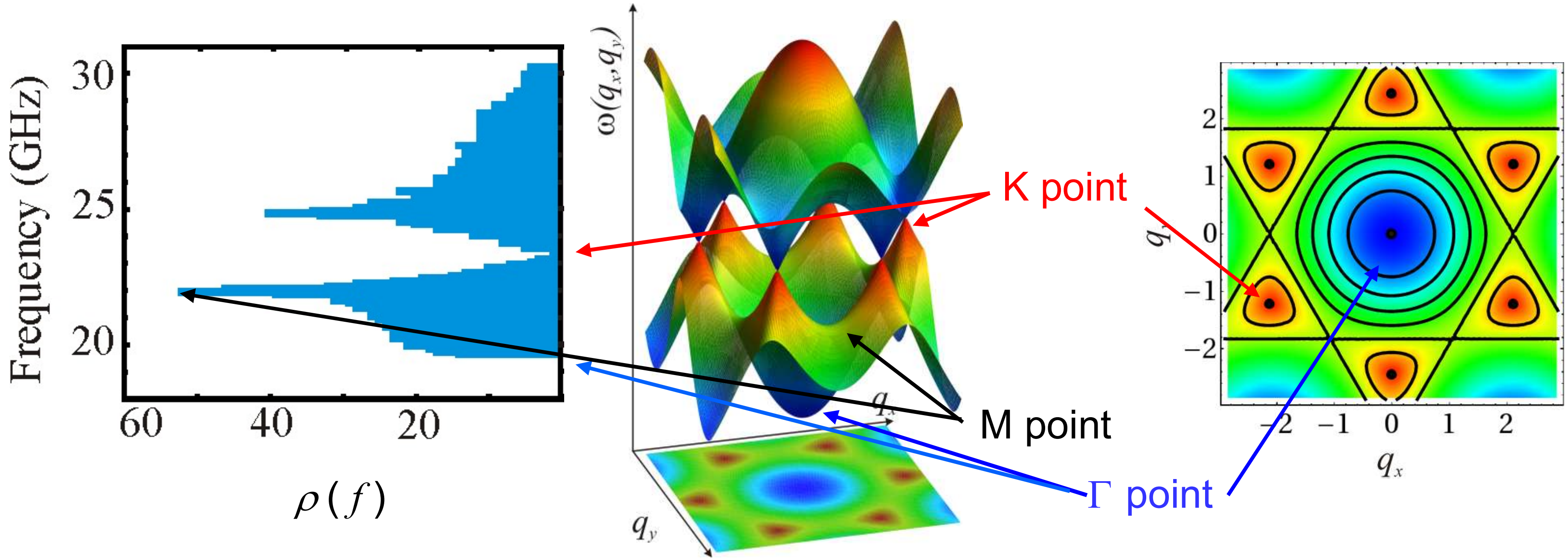

- Each resonance frequency f in the experimental DOS $\rho(f)$ is related to an isofrequency line of the band structure in quasimomentum (q) space
- Band edges: isofrequency lines form circles around the Γ point
- Sharp peaks: at frequencies of the saddle (M) points
- Broad minimum: at frequency of the Dirac (K) points

Center for Theoretical Physics of Complex Systems

Part III

Experiments with
Superconducting Microwave Resonators Simulating
Artificial Fullerene

B. Dietz, T. Klaus, M. Miski-Oglu, A. Richter, M. Wunderle
M. Bischoff, L. von Smekal, J. Wambach

Curved Graphene: Artificial Fullerene

Graphene flake

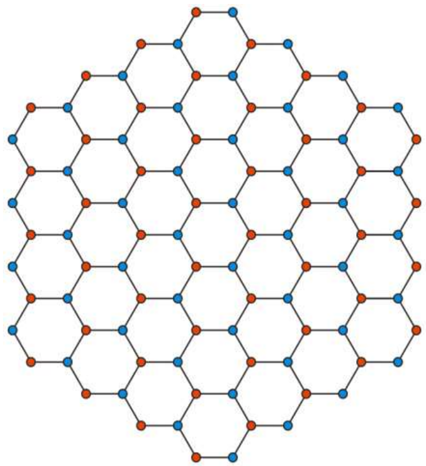

Curved graphene flake

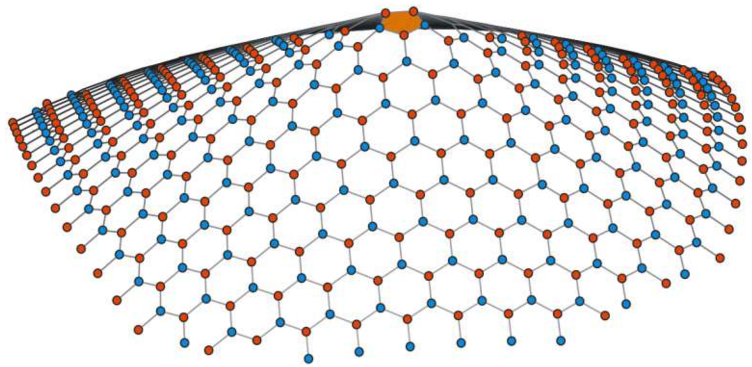

Fullerene C_{60}

- Curvature is introduced into graphene by replacing hexagons by pentagons
- Spherical fullerene molecules posses 12 pentagons
- Fullerene C_{60} (\`Buckyball´) consists of 12 pentagons and 20 hexagons arranged on a truncated icosahedron
- Low-energy electronic excitations are described by a Dirac equation on a sphere

Construction of Fullerene from a Plane Graphene Sheet

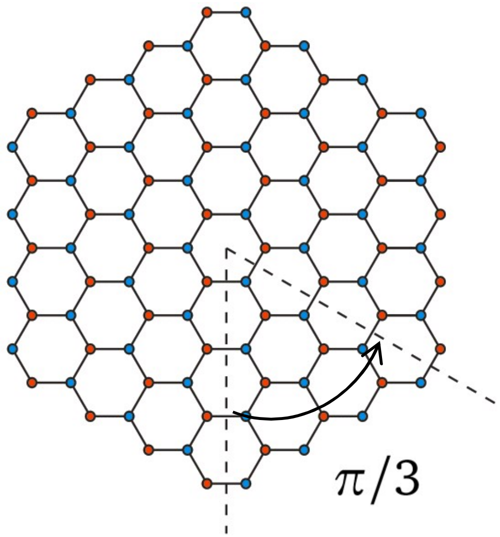

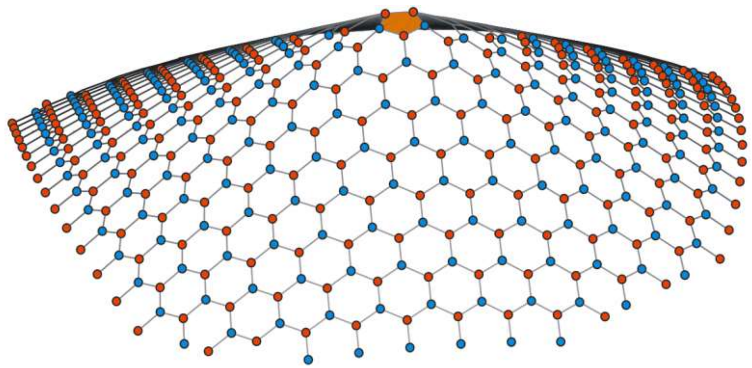

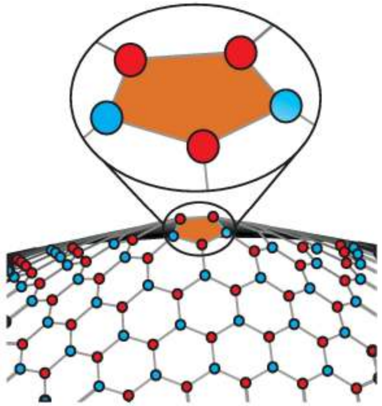

- To introduce the 12 pentagons, $\pi/3$ sectors are cut out and glued together
- Cones are created with the pentagon at the apex
- Transformation from a plane to a sphere implies changes in Dirac equation
- Mixing of the sublattices along the seam is accounted for by a gauge field A_μ producing a flux due to a magnetic monopole at the center of the fullerene
- The coordinate transformation associated with the curvature is accounted for by a quasi-spin connection Q_μ

Dirac Operators for Plane Graphene and Spherical Fullerene

- Dirac operator for plane graphene around the Dirac point

$$H_{\pm} = \pm v_F \, \sigma^{\alpha} \boxed{q_{\alpha}}, \; \alpha = x, y$$

- Dirac operator for spherical fullerene around the Dirac point

$$H_l = v_F \, \sigma^{\alpha} e^{\mu}_{\alpha} \left(\boxed{q_{\mu} - \underbrace{iQ_{\mu}}_{\text{curvature}} - \underbrace{iA^{l}_{\mu}}_{\text{sublattice mixing}}} \right), \; l=1,2$$

- Aim: experimental verification of the Atiyah-Singer index theorem
- Relates the topology of the carbon lattice to the number of zero modes, i.e., of eigenvalues of the Dirac operator at the Dirac point
- Plane graphene with periodic B.C.: no zero modes expected
- Spherical fullerene: a pair of triplets of (near) zero modes expected

Construction of the Superconducting Fullerene Microwave Billiard

- The structure of C_{60} was milled out from a brass ball and lead plated
- 60 circular cavities with radius 12 mm at the vertices of the truncated icosahedron
- 90 channels with width 14 mm at the edges of the truncated icosahedron
- Cut-off frequency of 1st (2nd) propagating mode: $f_c^1 \geq 10.714$ GHz ($f_c^2 \geq 20.232$GHz)
- All cavities / channels closed with triangular / rectangular plates
- Red caps mark antenna ports (altogether 8)
- 28 transmission spectra were measured

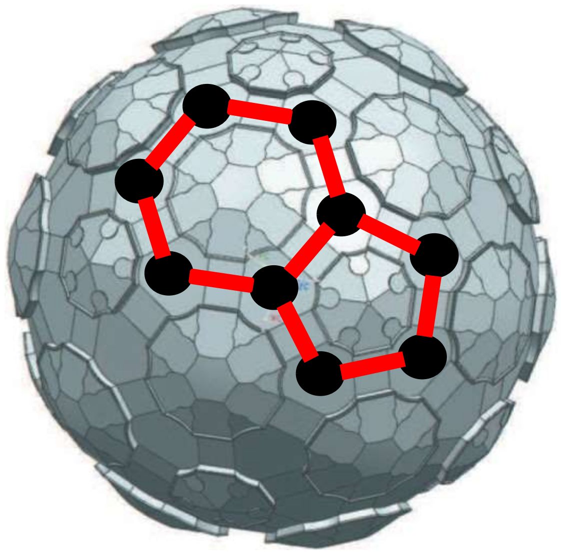

Construction of the Superconducting Fullerene Microwave Billiard

- The structure of C_{60} was milled out from a brass ball and lead plated
- 60 circular cavities with radius 12 mm at the vertices of the truncated icosahedron
- 90 channels with width 14 mm at the edges of the truncated icosahedron
- Cut-off frequency of 1st (2nd) propagating mode: $f_c^1 \geq 10.714$ GHz ($f_c^2 \geq 20.232$GHz)
- All cavities / channels closed with triangular / rectangular plates
- Red caps mark antenna ports (altogether 8)
- 28 transmission spectra were measured

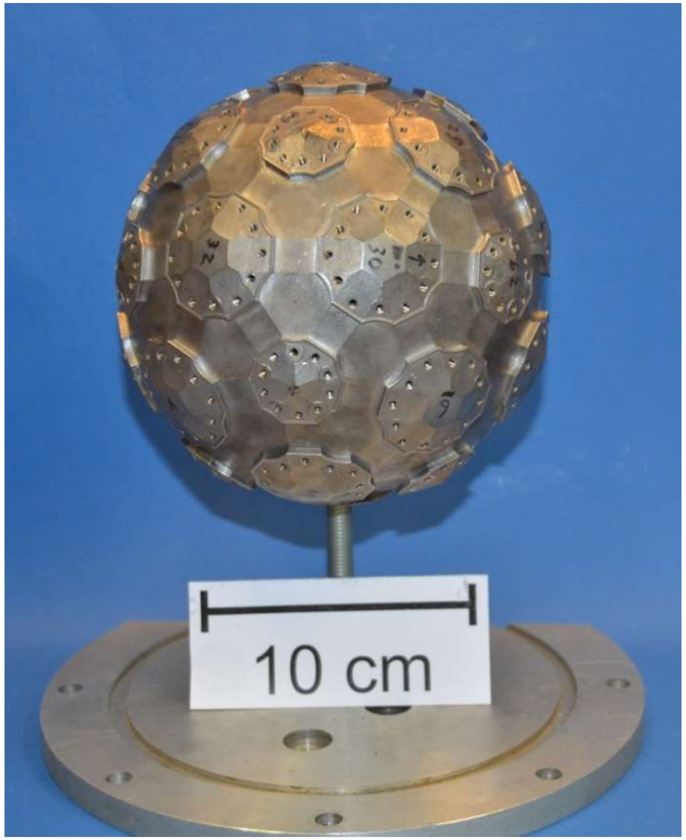

Construction of the Superconducting Fullerene Microwave Billiard

- The structure of C_{60} was milled out from a brass ball and lead plated
- 60 circular cavities with radius 12 mm at the vertices of the truncated icosahedron
- 90 channels with width 14 mm at the edges of the truncated icosahedron
- Cut-off frequency of 1st (2nd) propagating mode: $f_c^1 \geq 10.714$ GHz ($f_c^2 \geq 20.232$GHz)
- All cavities / channels closed with triangular / rectangular plates
- Red caps mark antenna ports (altogether 8)
- 28 transmission spectra were measured

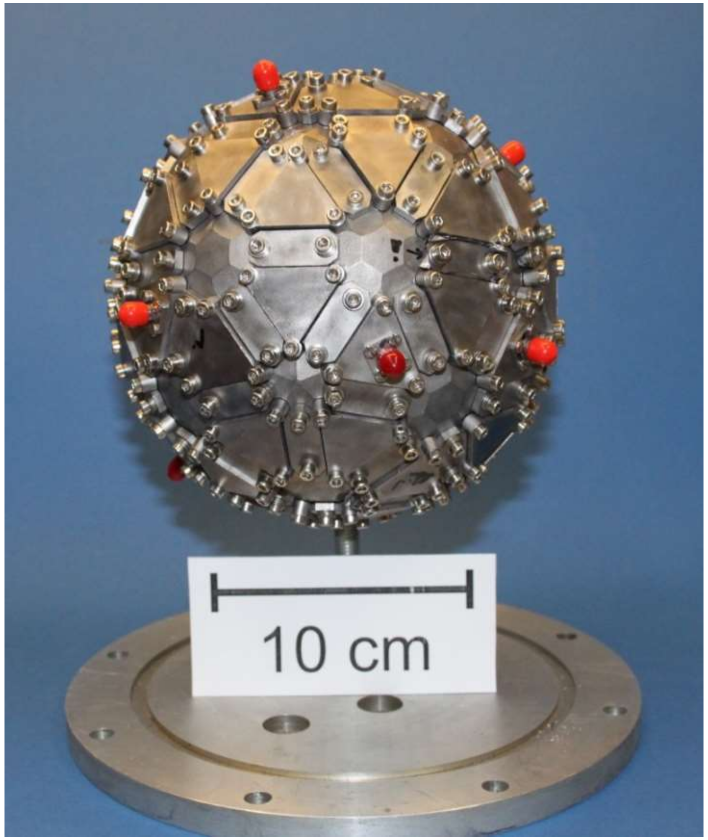

Spectrum of the Fullerene Billiard
[BD et al., PRL 115, 026801 (2015)]

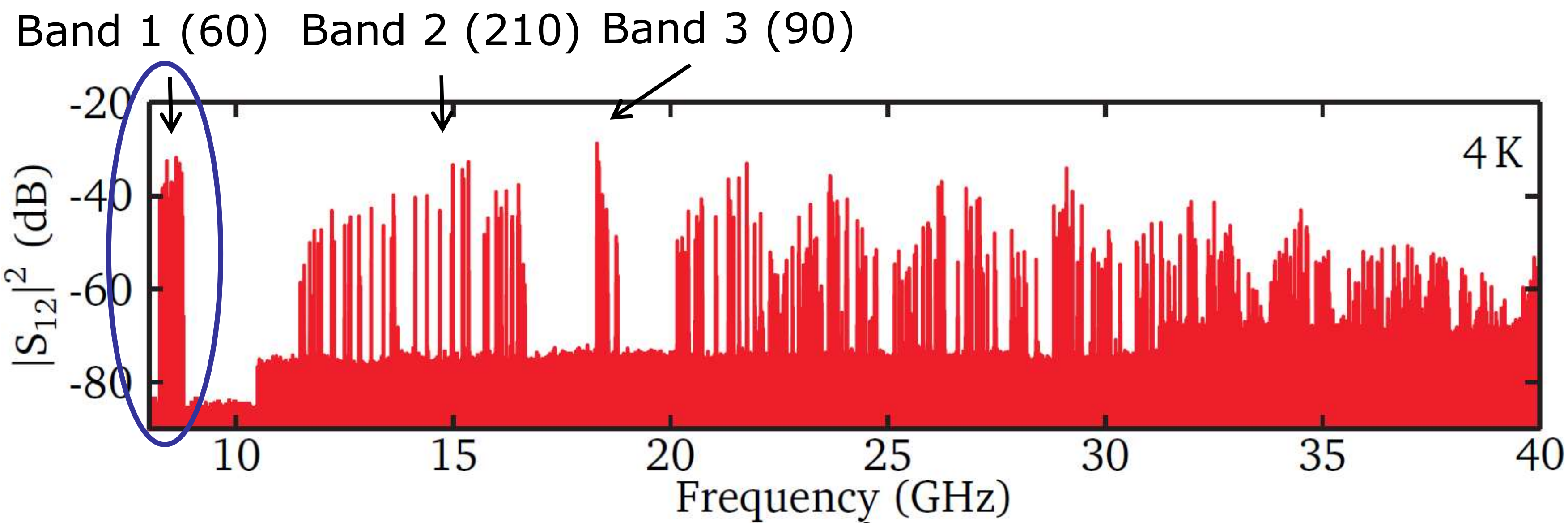

- Band 1: centered around 1st (J_0) mode of open circular billiard and below f_c^1 → modes in cavities weakly coupled to neighbors
- Band 2: centered around 2nd (J_1) mode of open circular billiard and above f_c^1 → mimicks a situation with an extra atom between neighboring C atoms
- Band 3: centered around 3rd (J_2) mode of open circular billiard and below f_c^2 → for symmetry reasons only 90 resonances
- Only the 1st band models the situation in C_{60}

PCS Center for Theoretical Physics of Complex Systems

Band 1

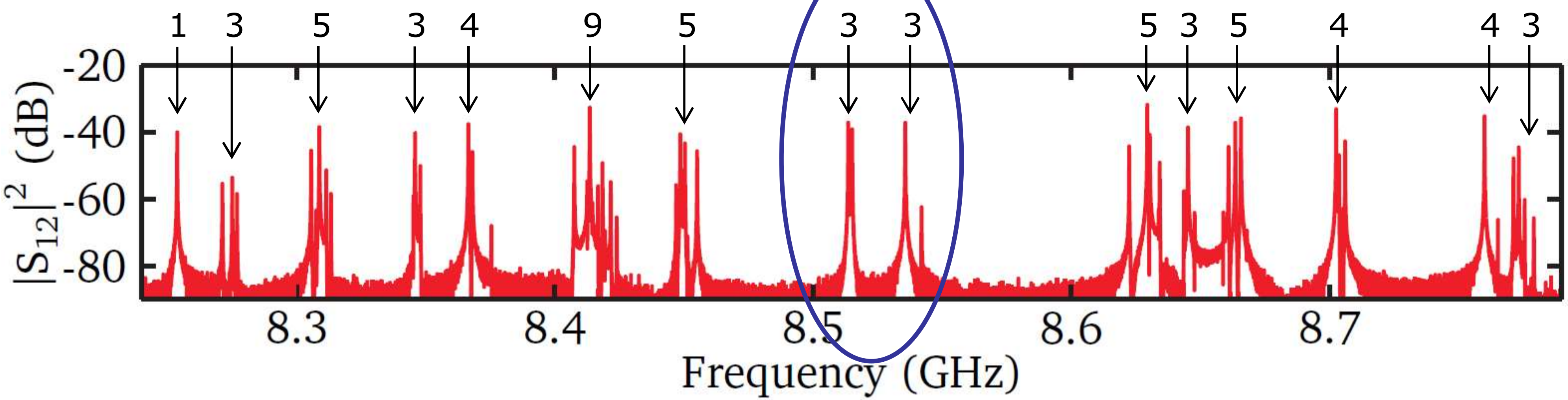

- Spectrum grouped into 15 multiplets and multiplicities agree with group theoretical predictions for the truncated icosahedral structure
- The degeneracies are lifted due to inhomogeneities of lead coating, i.e., changes in radii of cavities
- Dirac frequency is expected at the center of the first band, because of symmetry considerations (Manousakis PRB **44**,10991 (1991))
- There the Atiyah-Singer index theorem predicts 6 zero modes in the thermodynamic limit of an infinite number of C atoms

Zoom into Region Around the Center of Band 1

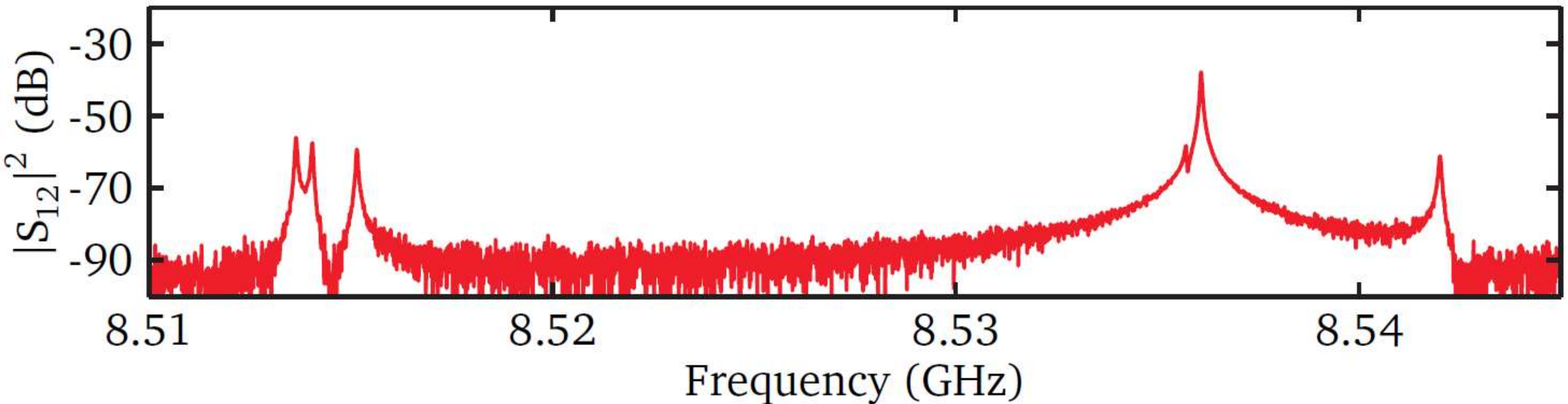

- Two triplets of nearly degenerate resonances
- Triplets correspond to resonances closest to the center of the spectrum

→ (near) zero modes predicted by Atiyah-Singer index theorem for a finite-size system?

- We corroborated this by matching the TBM to the experimental DOS and extrapolating it to larger fullerene molecules
- Agreement between experimental and calculated DOS best when including 1st, 2nd and 3rd nearest-neighbor couplings

Extrapolation of TBM Computations to Larger Fullerene Molecules

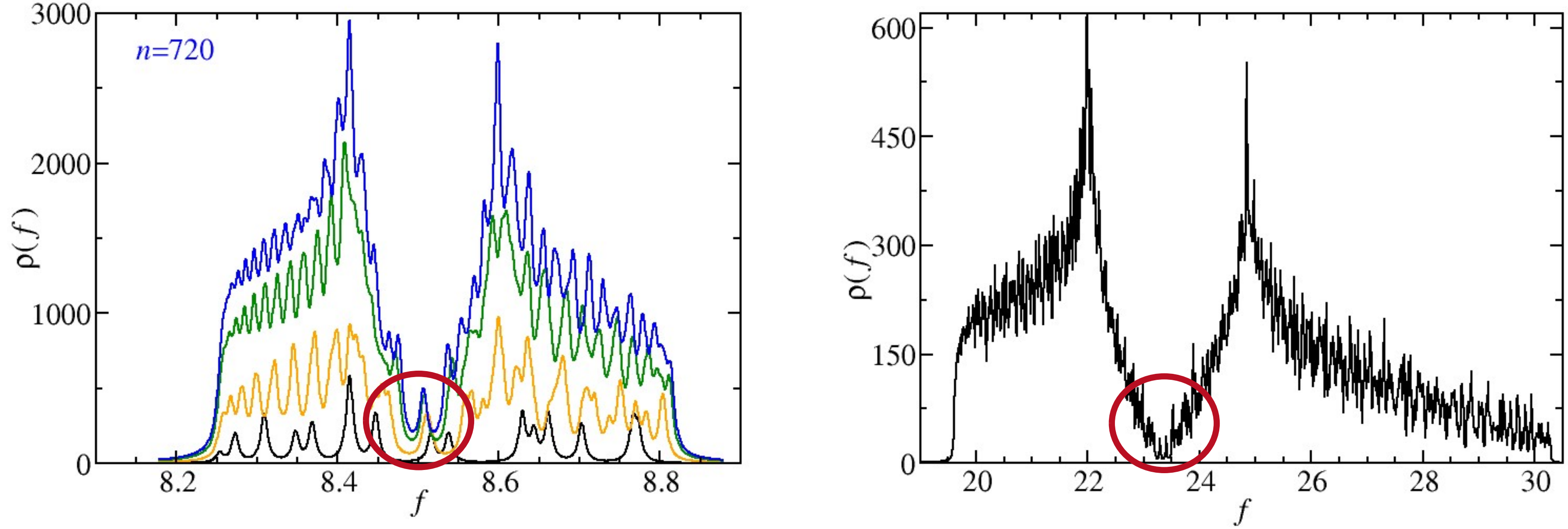

- N=60, 240, 540, 720
- DOS for C_n resembles more and more the DOS of the rectangular Dirac billiard with periodic boundary conditions
- One important difference: DOS of fullerene exhibits a peak at f_D due to the 2 triplets of (near) zero modes, that of graphene vanishes there

Central Frequency of Each Triplett Versus the Number n of C atoms

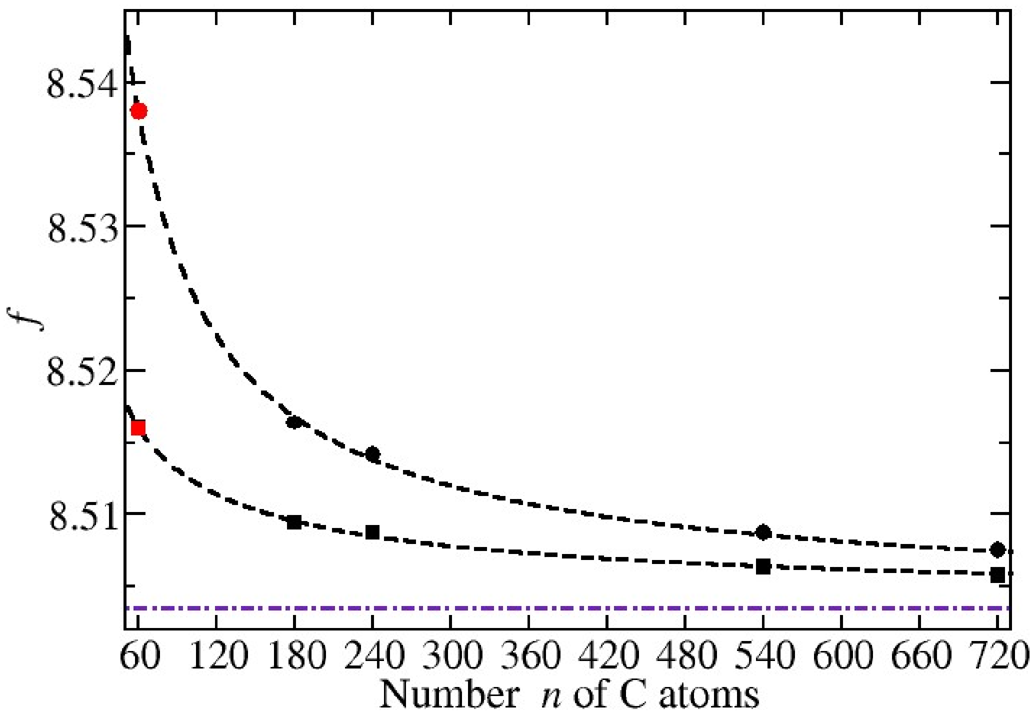

$: f(n) = f_D + a_0 / n^{a_1}$

- With increasing n the triplet frequencies converge towards the Dirac frequency f_D = 8.504 GHz

→ verifies the Atiyah-Singer theorem